Instruments and Observing Methods
Report No. 129

Report on the Second International Pyrgeometer Intercomparison (27 Sept - 15 Oct 2015, PMOD/WRC)

J. Gröbner and C. Thomann (Switzerland)

WEATHER CLIMATE WATER

WORLD
METEOROLOGICAL
ORGANIZATION

This publication is available in pdf format, from the WMO Library website:

https://library.wmo.int/opac/

© World Meteorological Organization, 2018

The right of publication in print, electronic and any other form and in any language is reserved by WMO. Short extracts from WMO publications may be reproduced without authorization, provided that the complete source is clearly indicated. Editorial correspondence and requests to publish, reproduce or translate this publication in part or in whole should be addressed to:

Chairperson, Publications Board
World Meteorological Organization (WMO)
7 bis, avenue de la Paix
P.O. Box 2300
CH-1211 Geneva 2, Switzerland

Tel.: +41 (0) 22 730 8403
Fax: +41 (0) 22 730 8040
E-mail: Publications@wmo.int

NOTE

The designations employed in WMO publications and the presentation of material in this publication do not imply the expression of any opinion whatsoever on the part of WMO concerning the legal status of any country, territory, city or area, or of its authorities, or concerning the delimitation of its frontiers or boundaries.

The mention of specific companies or products does not imply that they are endorsed or recommended by WMO in preference to others of a similar nature which are not mentioned or advertised.

The findings, interpretations and conclusions expressed in WMO publications with named authors are those of the authors alone and do not necessarily reflect those of WMO or its Members.

This publication has been issued without formal editing.

FOREWORD

The WMO Commission for Instruments and Methods of Observation (CIMO) as one of the eight Technical Commission of WMO focuses its work on accurate meteorological measurements by promoting and facilitating international standardization and compatibility of meteorological measurement systems used by Members within the WMO Integrated Global Observing System. Ensuring the traceability of meteorological measurements to agreed references has been at the core of its work to improve the quality of the products and services delivered by Members.

Precise and traceable radiation measurements are crucial to understanding the Earth's energy budget, and for monitoring changes in climate. The World Infrared Standard Group (WISG) was established to serve as interim reference for the calibration of pyrgeometers to ensure the world-wide comparability of the measurements of terrestrial infrared irradiance.

This second International Pyrgeometer Intercomparison (IPgC) was organized by the Physikalisch-Meteorologisches Observatorium Davos/World Radiation Centre (PMOD/WRC) in Davos, Switzerland. It permitted not only the characterization and calibration of a large number of instruments in a consistent manner, but it also confirmed the stability of several instruments that had been compared with the WISG at the 1st IPgC and other intercomparisons. Bringing the instruments together on a regular basis helps ensure all instruments remain traceable to a consistent reference, and that the WISG itself is stable. This intercomparison was also an occasion to assess the performance of new types of instruments that have or are being developed, and some of these have the potential to be used in the future as references directly traceable to the International System of Units (SI).

PMOD/WRC organized this intercomparison in parallel with two other instrument intercomparisons: the regularly occurring International Pyrheliometer Intercomparison (IPC) and the Filter Radiometer Comparison. This is a very efficient use of resources for those attending, and a unique opportunity for capacity development and sharing of experience amount the participants.

The results of IPgC have already provided important information for the future traceability of terrestrial irradiance measurements and were used at the recent special meeting of the CIMO Task Team on Radiation References in 2017 to plan investigations on terrestrial radiation traceability for routine network measurements. As a result, the Task Team has recommended that, like the IPC is for the World Radiometric Reference, future IPgC are part of the governance protocols of the WISG.

I wish to express my sincere gratitude and that of the WMO Commission for Instruments and Methods of Observation to the organizers of the IPgC, and authors of this report for their valuable work, as well as to all the staff of PMOD for supporting this intercomparison propagating the traceability of terrestrial infrared irradiance measurements to the WMO and broader radiation measurement community.

(Prof. B. Calpini)

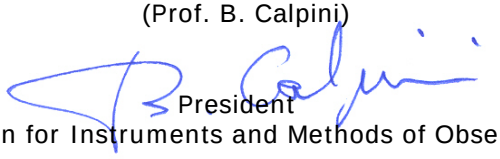

President
Commission for Instruments and Methods of Observation

Report of the second International Pyrgeometer Intercomparison from 27 September to 15 October 2015 at PMOD/WRC

Julian Gröbner, Christian Thomann
Physikalisch-Meteorologisches Observatorium Davos, World Radiation Centre (PMOD/WRC)
Infrared Radiometry Section (WRC-IRS)

1 Introduction 2
2 Setup and Instrumentation 2
3 Laboratory characterisation 4
4 Calibration relative to WISG 4
4.1 Stability of the WISG 5
5 Results 5
5.1 Blackbody versus WISG based calibration 7
5.2 PMOD versus Albrecht equation 7
5.3 Solar effect on unshaded pyrgeometers 8
6 IRIS, ACP and WISG 9
7 Conclusion 11
8 Annex 12

1 Introduction

The second international intercomparison of pyrgeometers (IPgC-II) was organised together with the twelfth International Pyrheliometer Comparison (IPC-XII) from 27 September to 15 October 2015 at the Infrared Radiometry Section (WRC-IRS) of the Physikalisch-Meteorologisches Observatorium Davos, World Radiation Centre (PMOD/WRC). 23 participants with a total of 38 pyrgeometers participated at this intercomparison. In addition, 5 IRIS radiometers (3 from PMOD/WRC, one from the Bureau of Meteorology (BOM), Australia and one from the Deutscher Wetterdienst (DWD), Germany, and 2 Absolute Cavity Pyrgeometer (ACP) from the National Renewable Energy Laboratory (NREL), United States of America, were used during three clear-sky nights in view of establishing a new reference for longwave irradiance measurements traceable to SI.

View of the measurement platform of WRC-IRS on top of the PMOD/WRC. The picture was taken facing East.

2 Setup and Instrumentation

The intercomparison took place at the PMOD/WRC, Switzerland, from 27 September to 15 October 2015. The outdoor measurement platform is located on the roof of the PMOD/WRC building at 1610 m.a.s.l., 46.8 N, 9.83 E. The measurement site is located in the Swiss Alps and its horizon is limited by mountains. Each pyrgeometer was characterised in the Blackbody of PMOD/WRC (Blackbody BB2007) to retrieve the pyrgeometer coefficients according to the standard PMOD formula. This procedure lasted for about 10 hours per instrument, so that the duration of the campaign was barely sufficient to cycle all instruments.

The pyrgeometers were installed on the measurement platform in ventilation units, on shaded and unshaded positions. The specific conditions for each pyrgeometer are described in Table 1. When not otherwise noted, pyrgeometers were placed in PMOD-VHS ventilation and heating units. Most pyrgeometers were connected to the PMOD data acquisition system (DAQ), apart from those denoted with “Operator”. The measured data were saved as one minute averages and regularly submitted to PMOD/WRC. A few instruments were initially operated on operator-controlled data acquisition systems, followed by a few days on the PMOD DAQ, as can be seen in Table 1.

The calibration of the participating pyrgeometers was performed according to the calibration procedure described in the IOM report No. 120 (WMO, 2015), using the World Infrared Standard Group of Pyrgeometers (WISG) as reference for atmospheric longwave irradiance.

Table 1. Participant information

Nb	Pyrgeometer	Type	DAQ	Institution	Remarks
1	PIR 31463F3	PIRmod	PMOD	PMOD/WRC	WISG1
2	PIR 31464F3	PIRmod	PMOD	PMOD/WRC	WISG2
3	CG4_FT004	CG4	PMOD	PMOD/WRC	WISG3
4	CG4_010535	CG4	PMOD	PMOD/WRC	WISG4
5	CG4_FT006	CG4	PMOD	PMOD/WRC	
6	CG4_060921	CG4	PMOD	BOM, Australia	
7	CGR4_140103	CGR4	PMOD	ASIAQ, Greenland	
8	IR20_105	IR20	PMOD	PMOD/WRC Hukseflux	No solarblind filter
9	IR20_103	IR20	PMOD	PMOD/WRC Hukseflux	
10	CGR4_110390	CGR4	PMOD	PMOD/WRC Kipp&Zonen	No solarblind filter
11	IR20_T2_4019	IR20	PMOD	Hukseflux, the Netherlands	
12	CG4_010536	CG4	PMOD	Kipp&Zonen, the Netherlands	
13	PIR 34007F3	PIR	PMOD	BOM, Australia	
14	CG4_050792	CG4	PMOD	SMHI, Sweden	SMHI Ventilation unit
15	PIR 28806F3	PIRmod	PMOD	Meteoswiss, Switzerland	
16	CG4_040736	CG4	PMOD	KNMI, the Netherlands	CVF3 Ventilation unit
17	CG4_060881	CG4	PMOD	NREL, US	
18	CGR4_100210	CGR4 PT100	PMOD	WMGO, Russia	
19	CG4_010567	CG4 PT100	PMOD	JMA, Japan	
20	CGR4_140016	CGR4 PT100	PMOD	SHMI, Slovakia	
21	CGR4_130648	CGR4	PMOD	CHMI, Czech Republic	
22	PIR_32227F3	PIR	PMOD	Eppley, US	
23	CGR4_130621	CGR4	PMOD	KACST, Saudi Arabia	CVF4 Ventilation unit
24	CG4_080066	CG4 PT100	PMOD	CENER, Spain	
25	CG4_030665	CG4	PMOD	CMA, China	
26	CGR4_140070	CGR4	PMOD	DMHZ, Croatia	
27	CGR4_100288	CGR4	PMOD	PUCC, Chile	
28	IR20_4018	IR20	PMOD	Nat. Cen. Univ. Taiwan	VU01 Ventilation unit
29	IR20_4020	IR20	PMOD	Nat. Cen. Univ. Taiwan	VU01 Ventilation unit
30	PIR_29143F3	PIR	PMOD	NOAA, US	
31	CGR4_110413	CGR4	Operator	Meteofrance, France	
32	IR20_4008	IR20	Operator	DWD, Germany	VU01 Ventilation unit. Measurements between 29 Sep. and 5 Oct. were affected by a clogged filter in the Ventilation unit.
33	IR20WS_5008	IR20	Operator	DWD, Germany	No solarblind filter, VU01 Measurements between 29 Sep. and 5 Oct. were affected by a clogged filter in the Ventilation unit.
34	CGR4_060027	CGR4 PT100	Operator	DWD, Germany	29 September-11 October Eigenbrodt SBL480 Ventilation unit
35	CG4_020617	CG4 PT100	Operator	DWD, Germany	Eigenbrodt SBL480 Ventilation unit.
36	PIR_30475F3	PIRmod	Operator	DWD, Germany	Eigenbrodt Ventilation unit
37	CGR4_060027	CGR4 PT100	PMOD	DWD, Germany	11 – 15 October
38	IR20_102	IR20	Operator	Hukseflux	29 Sep.-6 Oct., VU01
39	IR20_101	IR20	Operator	Hukseflux	VU01 Ventilation unit

3 Laboratory characterisation

Each pyrgeometer was characterised in the blackbody cavity BB2007 of PMOD/WRC (Gröbner, 2008). The characterisation procedure consisted in varying the blackbody temperature between +15 °C and -20 °C and the pyrgeometer body temperature between +20 °C and -10 °C to obtain 7 constant temperature levels at which the pyrgeometer coefficients C_{BB}, k_1, k_2, and k_3, were retrieved using the following equation:

$$E = \frac{U}{C_{BB}}\left(1 + k_1\sigma T_B^3\right) + k_2\sigma T_B^4 - k_3\sigma(T_D^4 - T_B^4) \quad (1)$$

where E is the irradiance in Wm^{-2}, U the pyrgeometer voltage in volt, and T_B and T_D the body and dome temperature respectively (called PMOD equation from now on). C, k_1, k_2, and k_3 are pyrgeometer specific coefficients which are retrieved for each pyrgeometer separately. The last term in equation 1 is set to zero for pyrgeometers without dome thermistor such as the CG4 type radiometers. For PIR pyrgeometers, the retrieval sensitivity of k_3 is significantly improved by differentially heating the dome of the pyrgeometer by a copper heating ring. This allows heating the dome by about +1 K relative to the body temperature.
The same measurements were used to retrieve the responsivity C and in case of Eppley PIR the dome coefficient K using the simplified version of equation 1 (often denoted Albrecht equation),

$$E = \frac{U}{C_{BB}} + \sigma T_B^4 - k_3\sigma(T_D^4 - T_B^4) \quad (2)$$

4 Calibration relative to WISG

The calibration of the participating pyrgeometers was performed according to the calibration procedure described in the IOM report No. 120 (WMO, 2015), against the WISG which served as reference for atmospheric longwave irradiance. Figure 1 shows the atmospheric downwelling longwave irradiance during the campaign. The data selection used to retrieve the sensitivity of the pyrgeometers used the following criteria:

1. Outliers are removed (U>0.001 V, U<-20 mV, $|T_D|$>40 °C, $|T_B|$>40 °C)
2. Any night containing rain is excluded (limit of 0.2 mm/10 min)
3. Stable atmospheric conditions, defined by the standard deviation of the WISG <2 Wm^{-2}
4. Net radiation measured by the WISG < -70 Wm^{-2}
5. Measurements from one night are used if there are at least 80% valid measurement points
6. Night is defined when the solar zenith angle is larger than 95°
7. Relative standard deviation of the test pyrgeometer signal <3%

Furthermore, as suggested in IOM report No. 120 (WMO, 2015), data is excluded from the calibration if the integrated water vapour (IWV), determined from the time delay of GPS receivers, is below 10 mm. The IWV varied between 4 mm and 20 mm during the campaign (see Figure 2).

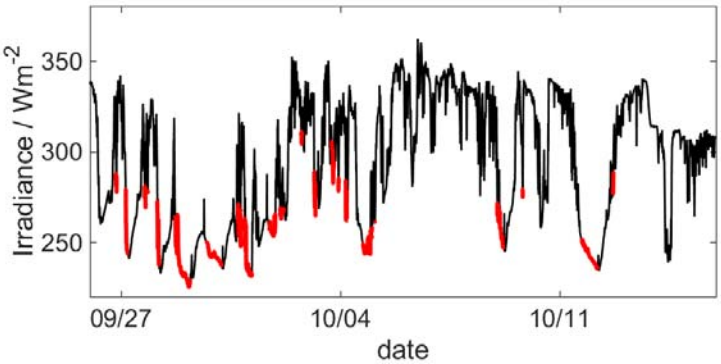

Figure 1. Downwelling longwave irradiance during the campaign. The red dots represent the data points which satisfy the calibration criteria.

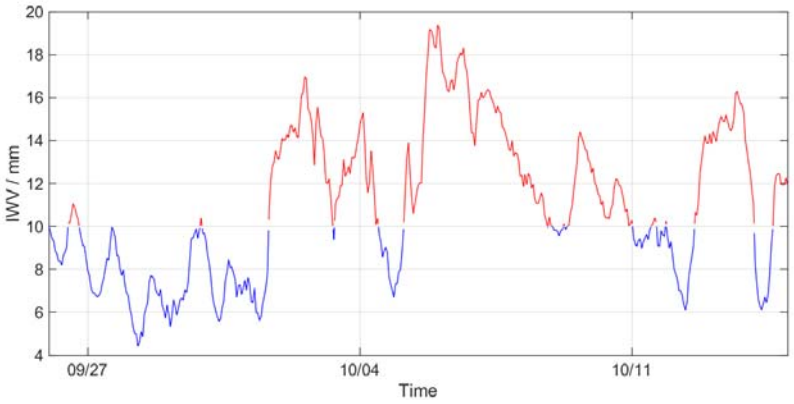

Figure 2. Integrated water vapour from GPS during the IPgC campaign. The threshold for using measurement data for the calibration is 10 mm (red curve). Nevertheless, the data for IWV less than 10 mm is still used for the comparison to the WISG.

4.1 Stability of the WISG

The WISG is operated continuously on the measurement platform of PMOD/WRC. Its stability is monitored by internal consistency checks of the four pyrgeometers comprising the WISG. As can be seen in Figure 3, the pyrgeometers of the WISG typically agree to within ± 1 Wm^{-2}, with minor seasonal variations between individual members of the WISG.

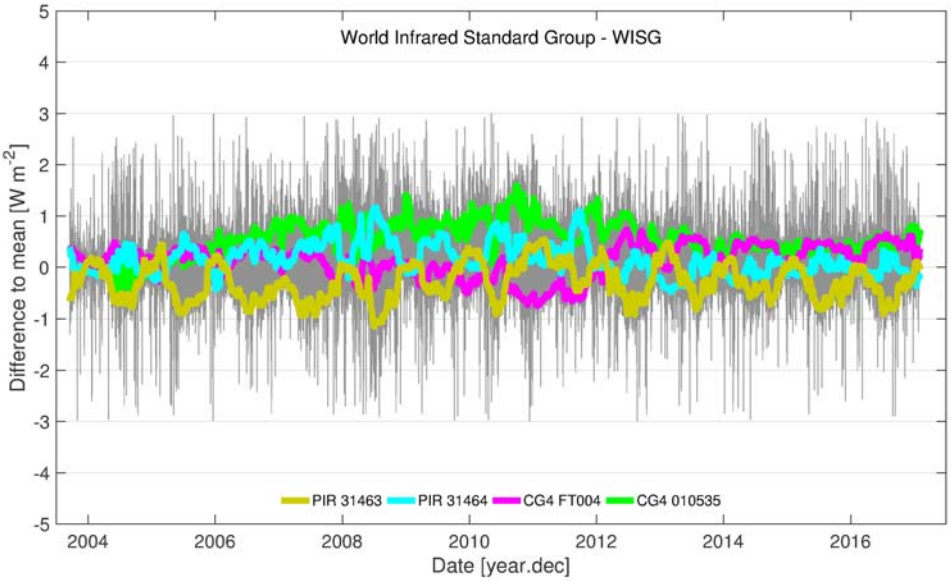

Figure 3. Night average differences of longwave irradiance measurements between the WISG pyrgeometers relative to their average. The thick lines represent a monthly running average.

5 Results

The results of the blackbody characterisation and the outdoor calibration relative to the WISG are summarised in Table 2. The coefficients k_1, k_2, k_3 and $C_{BLACKBODY}$ were retrieved with the blackbody as radiation source, while C_{WISG} was retrieved using k_1, k_2, k_3 and the atmospheric downwelling irradiance as source, as measured by the WISG. The responsivities C_{WISG} were retrieved using the PMOD (k_1, k_2, k_3) and Albrecht equations respectively. The figures showing the individual performance of each pyrgeometer are shown in the Annex at the end of this report.

Table 2. Results from the blackbody characterisation and the calibration relative to the WISG

Nb	Pyrgeometer	k_1	k_2	k_3	$C_{BLACKBODY}$		C_{WISG}		shaded/ unshaded
					k_1, k_2, k_3	Albrecht	k_1, k_2, k_3	Albrecht	
1	PIR 31463F3	0.044	0.9952	3.2	3.617	3.325	3.770	3.506	S
2	PIR 31464F3	-0.014	0.9943	2.7	3.698	3.628	3.764	3.741	S
3	CG4_FT004	-0.058	0.9974	0	11.463	12.142	12.036	12.814	S
4	CG4_010535	-0.037	0.9979	0	8.913	9.013	9.388	9.743	S
5	CG4_FT006	0.066	1.0000	0	11.896	11.000	11.559	10.701	S
6	CG4_060921	0.036	0.9991	0	8.687	8.267	8.409	8.023	U
7	CGR4_140103	0.000	1.0000	0	12.020	12.020	11.807	11.807	S
8	IR20_105	-0.047	1.0006	0	15.300	16.294	14.798	15.739	U
9	IR20_103	-0.059	0.9988	0	17.000	18.174	17.832	19.122	U
10	CGR4_110390	-0.001	0.9989	0	8.833	8.871	8.406	8.379	U
11	IR20_T2_4019	-0.138	0.9988	0	6.870	8.280	7.156	8.553	S
12	CG4_010536	0.021	0.9976	0	9.382	9.000	9.172	8.854	S
13	PIR 34007F3	0.076	1.0000	4.02	3.654	3.342	4.037	3.695	S
14	CG4_050792	0.043	0.9992	0	8.853	8.363	8.609	8.150	U
15	PIR 28806F3	0.249	1.0081	3.2	4.210	3.397	4.439	3.522	S
16	CG4_040736	0.013	0.9994	0	12.620	12.364	12.254	12.032	U
17	CG4_060881	0.024	0.9978	0	8.390	8.024	8.315	8.004	U
18	CGR4_100210	0.012	0.9988	0	10.401	10.162	10.256	10.057	U
19	CG4_010567	0.014	0.9975	0	11.004	10.632	12.303	11.971	U
20	CGR4_140016	-0.020	0.9998	0	11.179	11.432	10.654	10.912	S
21	CGR4_130648	0.000	0.9993	0	10.800	10.770	10.860	10.828	U
22	PIR_32227F3	-0.035	0.9962	2.7	3.796	3.870	3.869	3.981	S
23	CGR4_130621	-0.032	0.9984	0	11.620	11.968	11.268	11.653	U
24	CG4_080066	0.050	0.9989	0	14.453	13.522	14.162	13.282	U
25	CG4_030665	0.035	0.9995	0	11.458	10.943	11.169	10.685	U
26	CGR4_140070	-0.018	0.9984	0	11.080	11.210	11.060	11.236	U
27	CGR4_100288	0.028	0.9989	0	7.356	7.058	7.183	6.913	U
28	IR20_4018	-0.111	0.9993	0	17.250	19.930	18.266	21.136	U
29	IR20_4020	-0.142	0.9990	0	6.648	8.031	7.016	8.493	U
30	PIR_29143F3	0.310	1.0044	3.9	4.588	3.414	4.659	3.426	U
*31	CGR4_110413	0.0341	0.9999	0	9.987	9.577	9.878	9.480	U
*32	IR20_4008	-0.124	0.9953	0	18.860	21.602	19.761	23.314	U
*33	IR20WS_5008	-0.137	0.9652	0	16.492	15.837	16.468	18.106	U
*34	CGR4_060027a	0.016	1.0000	0	14.945	14.658	14.679	14.397	U
*35	CG4_020617	0.041	0.9977	0	12.335	11.560	13.627	12.849	U
*36	PIR_30475F3	0.061	1.0011	3.8	3.743	3.504	4.031	3.770	U
37	CGR4_060027b	0.016	1.0000	0	14.945	14.658	14.752	14.469	U
*38	IR20_102b	-0.104	0.9984	0	17.115	19.463	17.662	20.169	U
*39	IR20_101	-0.103	0.9993	0	16.664	18.980	17.255	19.705	U

5.1 Blackbody versus WISG based calibration

As shown in previous studies, atmospheric downwelling irradiance measurements from pyrgeometers which are based on blackbody based calibrations show large differences. These differences can be quantified from the responsivities C_{WISG} and $C_{BLACKBODY}$. The relative difference between the two responsivities can be directly expressed in Wm^{-2} by multiplying the relative difference by a net irradiance of -100 Wm^{-2}, typical for clear sky conditions. Figure 4 shows the relative difference between C_{WISG} and $C_{BLACKBODY}$ expressed in %.

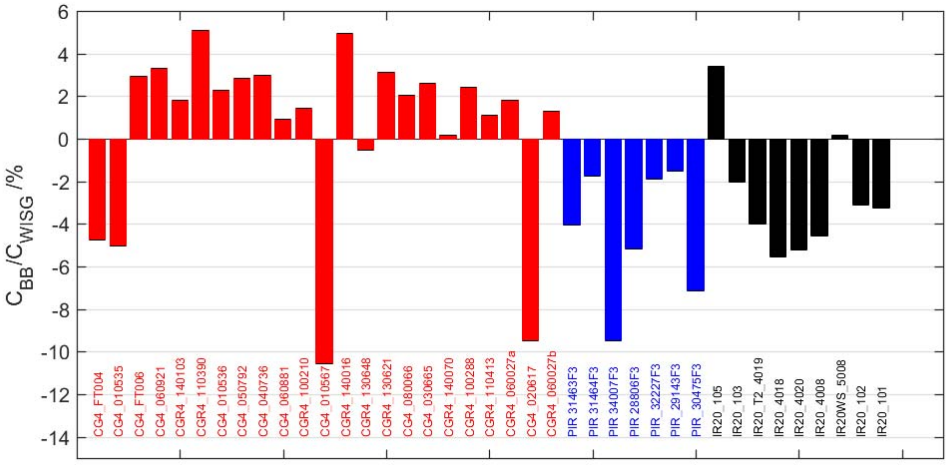

Figure 4. Relative differences between the blackbody based and WISG based responsivities. The red, blue and black bars represent the Kipp&Zonen CG4/CGR4, Eppley PIR and Hukseflux IR20 pyrgeometers respectively.

As can be seen in Figure 4, differences of up to 15 Wm^{-2} can be expected between clear sky atmospheric longwave irradiance measurements from pyrgeometers calibrated in the same blackbody. As discussed in previous studies, these differences are assumed to arise from the spectral mismatch of the spectral dome transmissions and the spectral differences between the blackbody radiation and the atmospheric downwelling radiation.

5.2 PMOD versus Albrecht equation

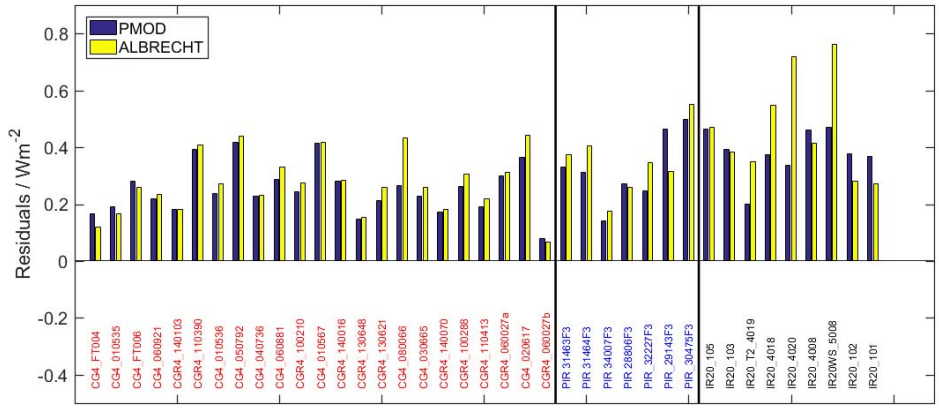

Figure 5. Calibration residuals (standard deviation) using the PMOD or Albrecht equation for night-time data only.

The standard deviation of the residuals from the outdoor calibration relative to the WISG are shown in Figure 5 for the PMOD and Albrecht equations. As can be seen in the figure, the residuals from the PMOD equation are usually smaller than when using the Albrecht equation, even though for some instruments the opposite is also seen. On average, CG4 type pyrgeometers show the lowest residuals with respect to the WISG, followed by PIR and Hukseflux IR20 pyrgeometers (see Table 3).

Table 3. Standard deviation of the calibration residuals per instrument type.

Instrument	Residuals in Wm^{-2}	
	PMOD	Albrecht
CG4/CGR4	0.25	0.27
PIR	0.32	0.35
IR20	0.40	0.48

The PMOD equation performs about 10% better than the Albrecht equation for the CG4 and PIR pyrgeometers, while for the IR20 the improvement is nearly 20%. This is due to the fact that IR20 pyrgeometers do not include a temperature compensation circuitry, but need a temperature correction which is included in the PMOD equation through the k_1 coefficient (see equation 1) or by applying a temperature correction as suggested by the manufacturer.

5.3 Solar effect on unshaded pyrgeometers

The solar influence on pyrgeometer measurements was determined from daily data by correlating the residuals between the individual unshaded pyrgeometers to the shaded WISG with the direct shortwave solar irradiance converted to horizontal incidence (see figures in annex). The quoted solar bias in the figure below is then determined for nominal 1000 W direct solar irradiance (weighted on the receiver) by linearly extrapolating the residuals for each instrument.

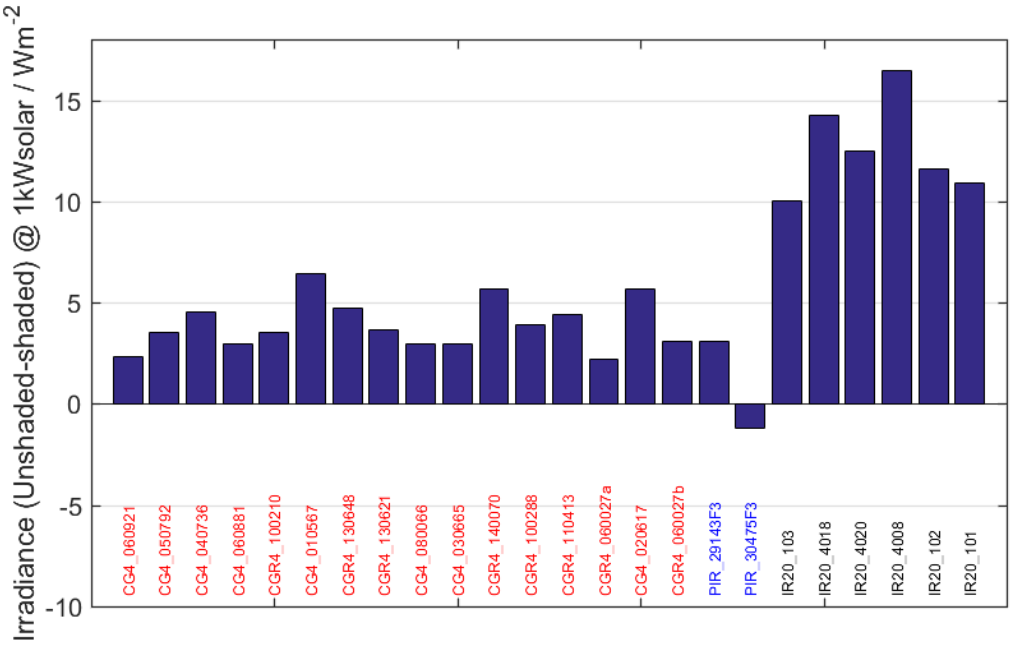

Figure 6. Solar influence on daytime pyrgeometer measurements. The values are quoted for direct solar irradiance of 1 kW on a horizontal surface.

The average solar influence on the different pyrgeometer types is 3.6 Wm^{-2} and 12.2 Wm^{-2} for the CG4 and IR20 pyrgeometers respectively. There were not enough Eppley PIR pyrgeometers measuring in an unshaded position to provide any statistics. The slightly negative value of PIR 30475F3 is not significant.

6 IRIS, ACP and WISG

Four IRIS and 2 ACP absolutely calibrated longwave infrared radiometers took part in the IPgC. Due to their windowless operation, measurements were only available during nights without precipitation: 22 September was a nearly complete cloud free night, while 26 September was fully overcast. On 29, 30 September and 12 October, IRIS and ACP measured simultaneously during cloud free conditions.
The IRIS radiometers provide irradiance values averaged over 10 seconds, the WISG 1 minute averages and the ACP every 30 seconds.
The Figures 7 to 10 show the residuals between the irradiance measurements by the individual radiometers as well as the WISG to the IRIS average.

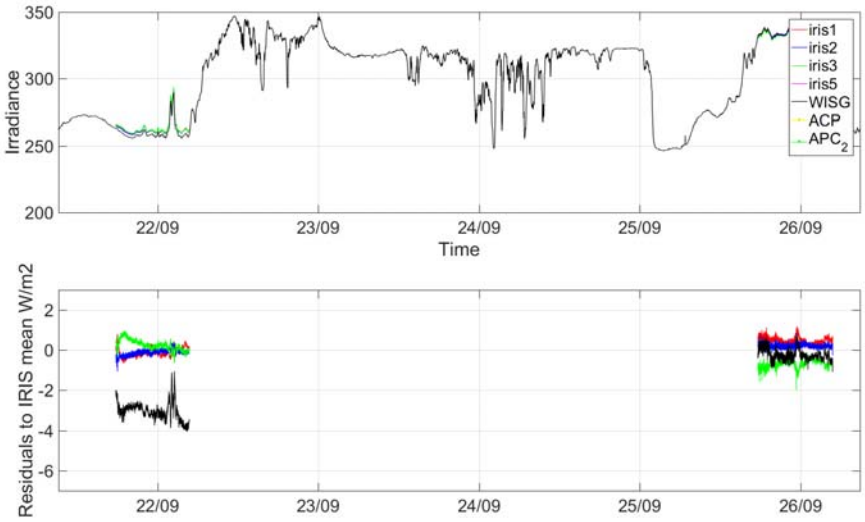

Figure 7. Longwave irradiance measurements for the nights of 21 to 22 September and 25 to 26 September when only IRIS 1, 2, 3 and the WISG were present (top). Difference to average of IRIS 1, 2, 3 (bottom).

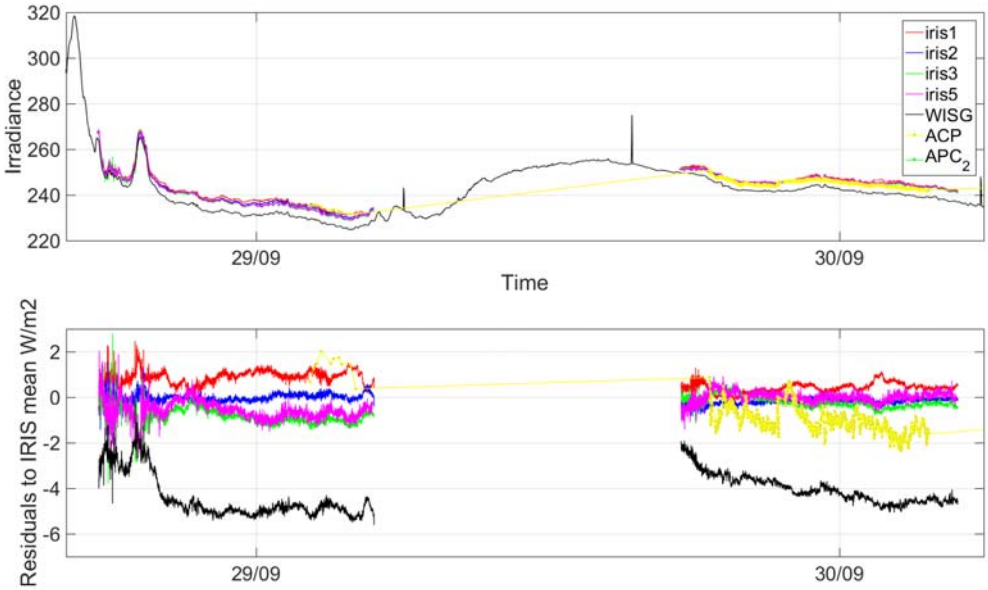

Figure 8. Longwave irradiance measurements for the nights of 28 to 29 September and 29 to 30 September with IRIS 1, 2, 3, 5, the ACP and the WISG (top). Difference to average of IRIS 1, 2, 3 (bottom).

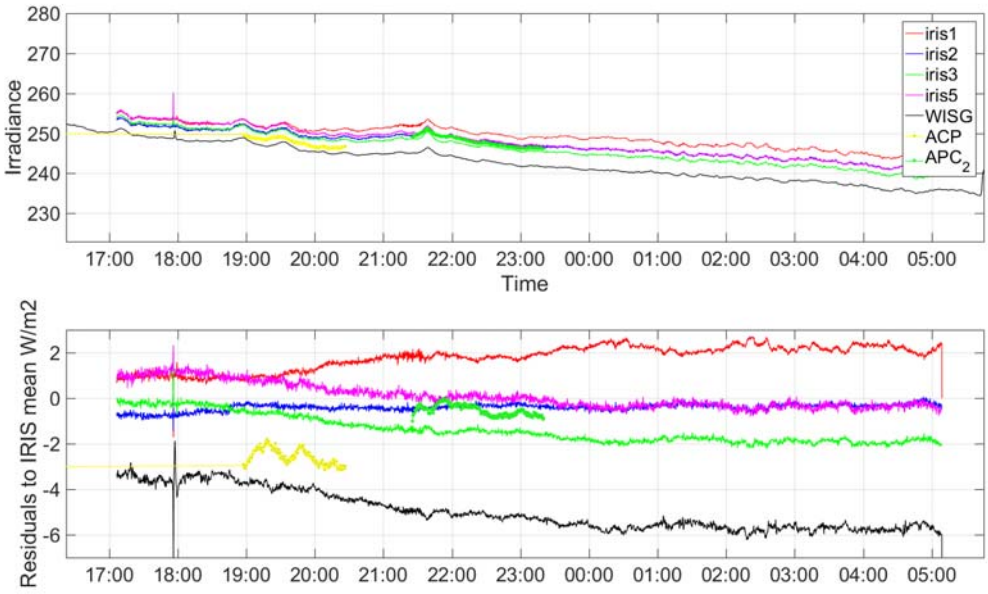

Figure 9. Longwave irradiance measurements for the night of 11 to 12 October with IRIS 1, 2, 3, 5, the ACP-1 and ACP-2 and the WISG (top). Difference to average of IRIS 1, 2, 3 (bottom).

As seen in the figures, the IRIS and ACP radiometers measure between 3 Wm^{-2} to 6 Wm^{-2} higher irradiance than the WISG during cloud free nights. During overcast conditions (25 September and the evening of 28 September) the WISG and the IRIS agree much better, indicating that the differences arise from the net downwelling longwave irradiance.

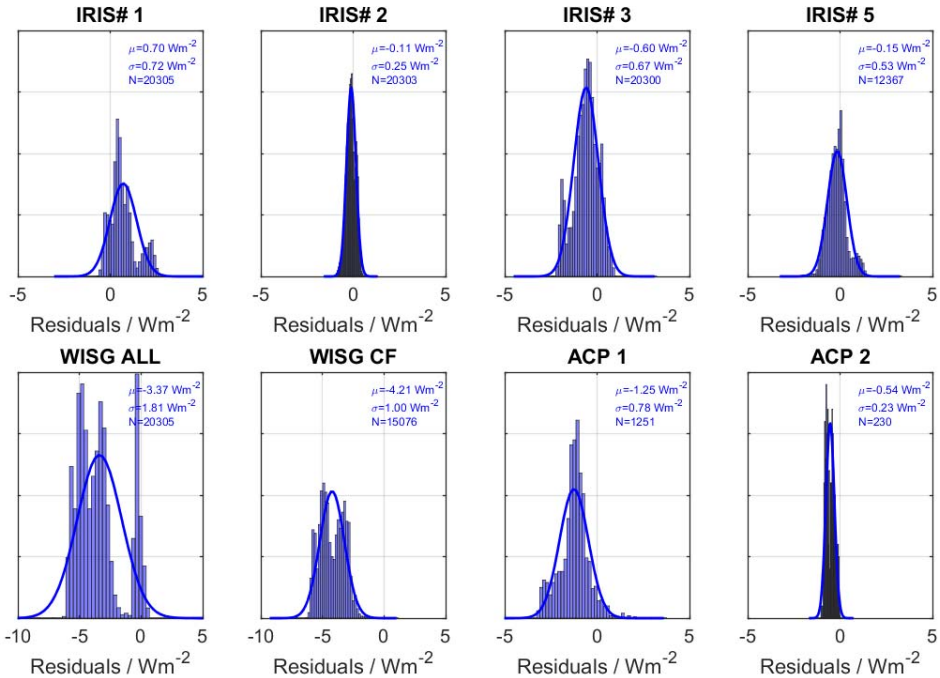

Figure 10. Residuals between the radiometers and the average of the IRIS 1, 2, 3 for the selected days shown in the previous figures.

As can be seen in Figure 10, the IRIS radiometers agree well with each other, with average differences between -0.6 Wm^{-2} to +0.7 Wm^{-2}. The WISG shows a distinct double peak, which comes from the difference between overcast and cloud free periods. During cloud-free periods, the average

difference is -4.2 Wm^{-2}. The ACP radiometers have less measurements, but they clearly group with the IRIS radiometers, at -1.25 Wm^{-2} for ACP-1 and -0.54 Wm^{-2} for ACP-2.

7 Conclusion

1) The WISG has been measuring continuously since 2004. Between 2004 and 2015, the four pyrgeometers comprising the WISG show an internal consistency of 1 Wm^{-2}, demonstrating that the WISG can be used as a stable reference for longterm atmospheric longwave irradiance measurements.

2) As shown in this IPgC, pyrgeometers can be calibrated relative to an outdoor reference like the WISG with an expanded uncertainty of less than 1 Wm^{-2} with a 95% coverage probability.

3) The solar influence of unshaded pyrgeometers is correlated to the incoming direct solar irradiance and can be as high as 12 Wm^{-2} for 1000 W horizontal direct solar irradiance.

4) Atmospheric longwave irradiance measurements can give discrepancies of up to 15 Wm^{-2} between instruments calibrated in the same blackbody cavity.

5) Atmospheric longwave irradiance measurements of the IRIS and ACP absolute radiometers give consistent results to within 1.5 Wm^{-2}, which is well within their stated uncertainties. The difference between ACP, IRIS and the WISG is 4.2 Wm^{-2} during cloud free nights, with WISG measuring lower. These results are consistent with previous findings as published in Gröbner et al., 2014.

Reference

Gröbner, J., 2008: Operation and Investigation of a tilted bottom cavity for pyrgeometer characterizations, *Applied Optics.*, 47:4441-4447.

Gröbner, J., I. Reda, S. Wacker, S. Nyeki, K. Behrens, and J. Gorman, 2014: A new absolute reference for atmospheric longwave irradiance measurements with traceability to SI units, *J. Geophys. Res. Atmos.*, 119, doi:10.1002/2014JD021630.

World Meteorological Organization, 2015: Pyrgeometer calibration procedure at the PMOD/WRC-IRS (J. Gröbner and S. Wacker). Instruments and Observing Methods Report No. 120. Geneva.

Acknowledgments

The authors would like to thank those participants who operated their instruments on their own data acquisition system and for providing their data. Thanks also to T. Carlund, S. Wacker, I. Reda, B. Forgan, J. Konings, C. Donkers, and N. Ohkawara for helpful discussions and comments to an early version of the report.

Annex

Measurement results for individual pyrgeometers.
DUT – Device under Test

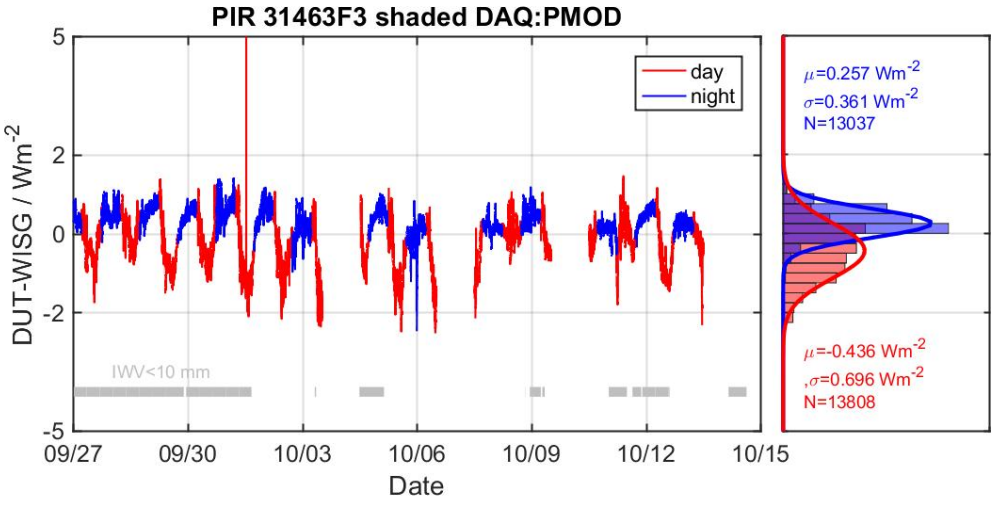
PIR 31463F3 shaded DAQ:PMOD
day
night
IWV<10 mm
DUT-WISG / Wm-2
Date
09/27
09/30
10/03
10/06
10/09
10/12
10/15
μ=0.257 Wm-2
σ=0.361 Wm-2
N=13037
μ=-0.436 Wm-2
,σ=0.696 Wm-2
N=13808

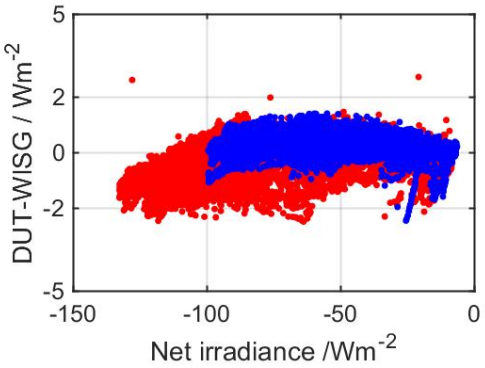
DUT-WISG / Wm-2
Net irradiance /Wm-2

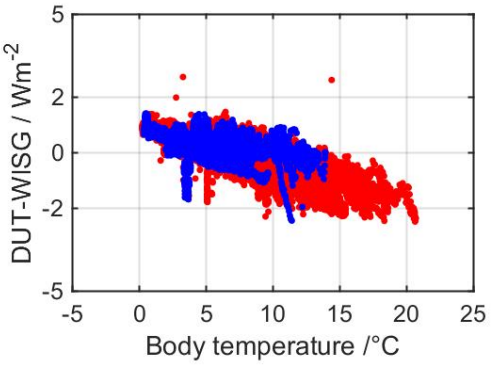
DUT-WISG / Wm-2
Body temperature /°C

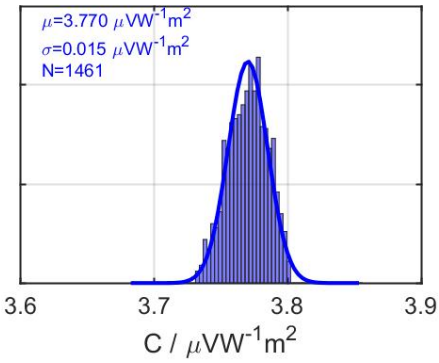
μ=3.770 μVW-1m2
σ=0.015 μVW-1m2
N=1461
C / μVW-1m2

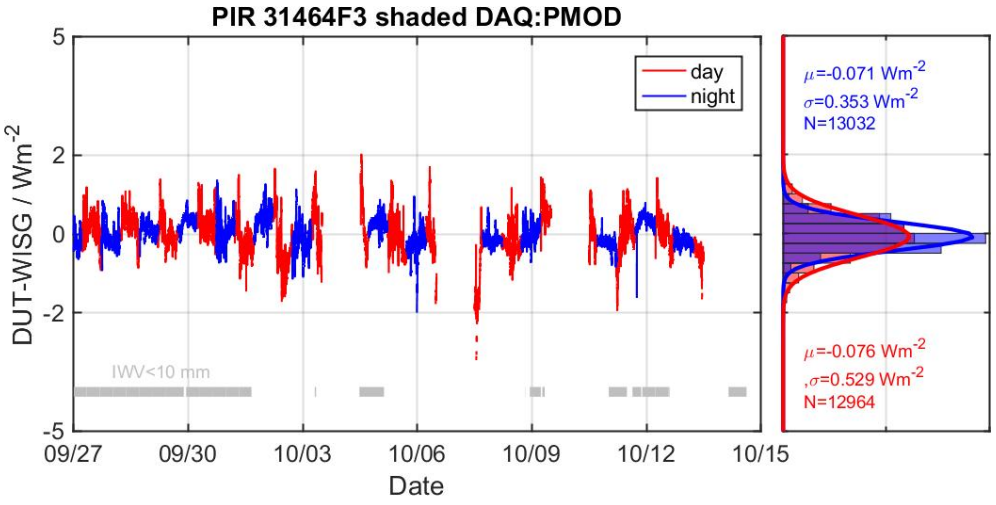
PIR 31464F3 shaded DAQ:PMOD
day
night
IWV<10 mm
DUT-WISG / Wm-2
Date
09/27
09/30
10/03
10/06
10/09
10/12
10/15
μ=-0.071 Wm-2
σ=0.353 Wm-2
N=13032
μ=-0.076 Wm-2
,σ=0.529 Wm-2
N=12964

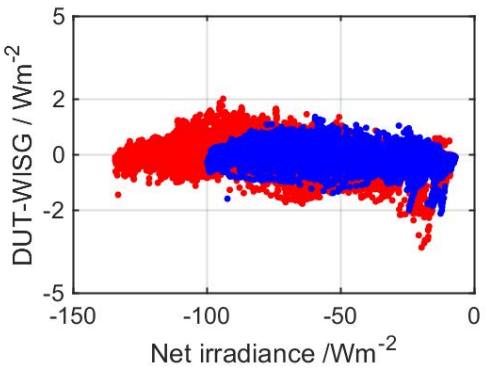
DUT-WISG / Wm-2
Net irradiance /Wm-2

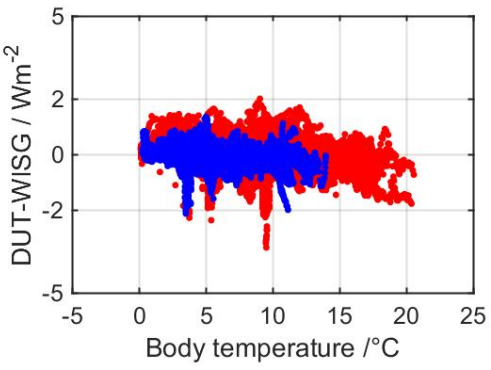
DUT-WISG / Wm-2
Body temperature /°C

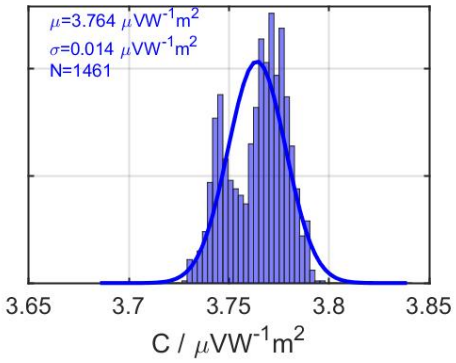
μ=3.764 μVW-1m2
σ=0.014 μVW-1m2
N=1461
C / μVW-1m2

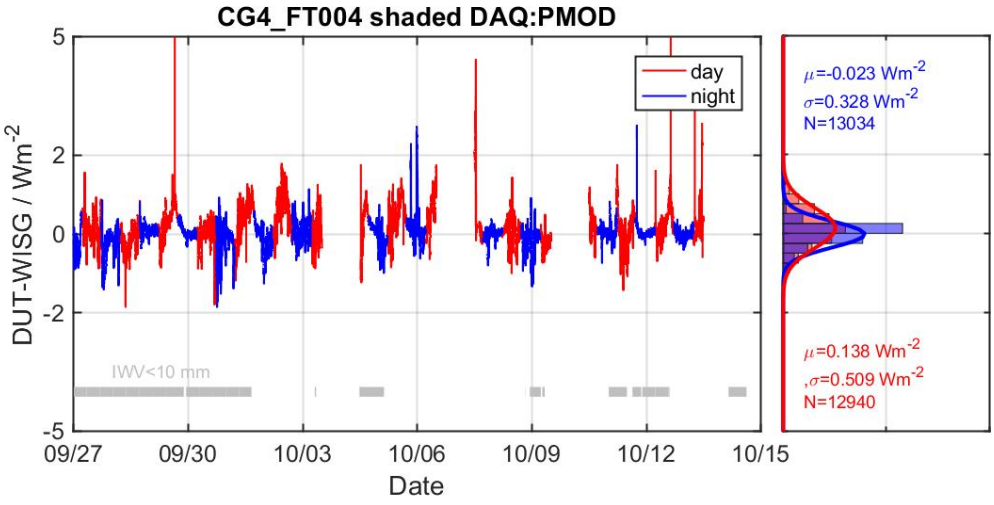
CG4_FT004 shaded DAQ:PMOD
day
night
IWV<10 mm
DUT-WISG / Wm-2
Date
09/27
09/30
10/03
10/06
10/09
10/12
10/15
μ=-0.023 Wm-2
σ=0.328 Wm-2
N=13034
μ=0.138 Wm-2
,σ=0.509 Wm-2
N=12940

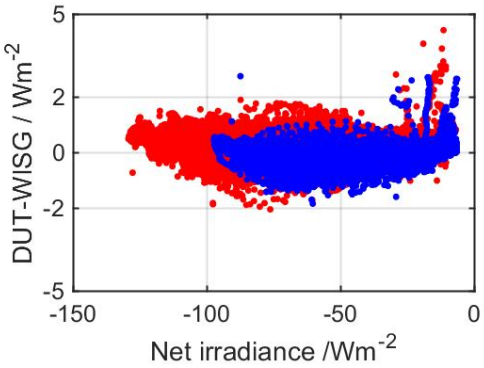
DUT-WISG / Wm-2
Net irradiance /Wm-2

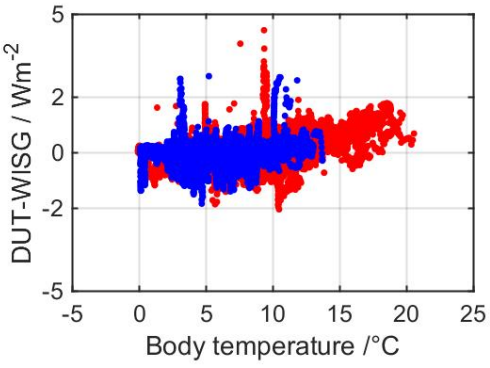
DUT-WISG / Wm-2
Body temperature /°C

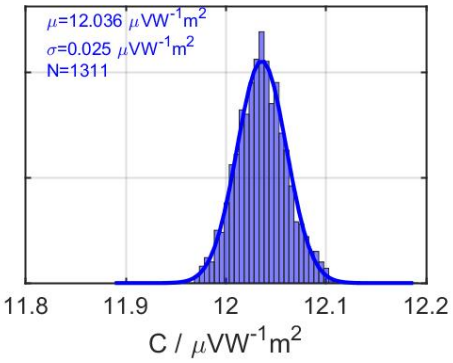
μ=12.036 μVW-1m2
σ=0.025 μVW-1m2
N=1311
C / μVW-1m2

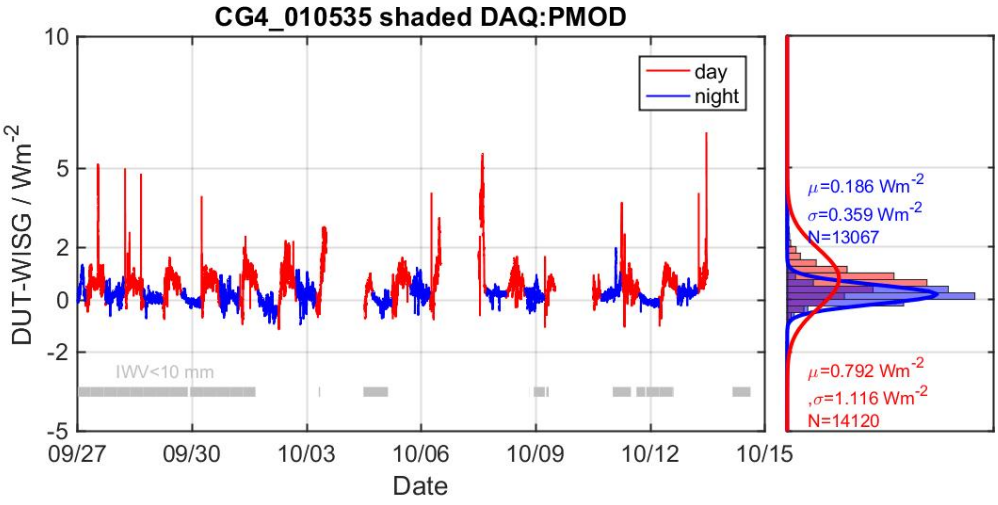
CG4_010535 shaded DAQ:PMOD
day
night
DUT-WISG / Wm-2
IWV<10 mm
09/27
09/30
10/03
10/06
10/09
10/12
10/15
Date
μ=0.186 Wm-2
σ=0.359 Wm-2
N=13067
μ=0.792 Wm-2
,σ=1.116 Wm-2
N=14120

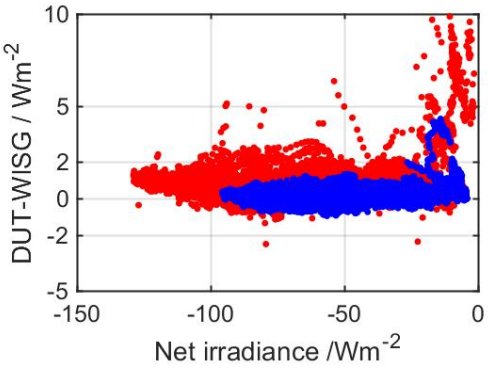
DUT-WISG / Wm-2
Net irradiance /Wm-2

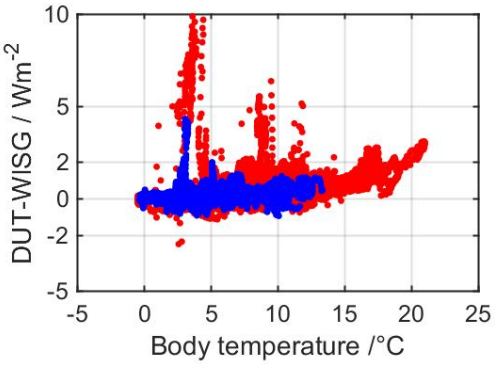
DUT-WISG / Wm-2
Body temperature /°C

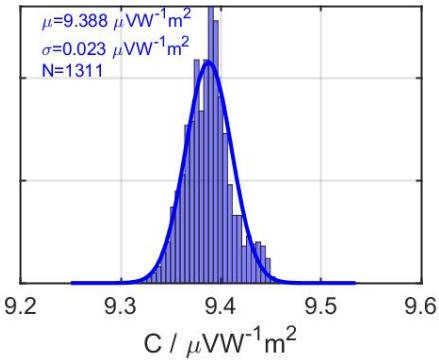
μ=9.388 μVW-1m2
σ=0.023 μVW-1m2
N=1311
C / μVW-1m2

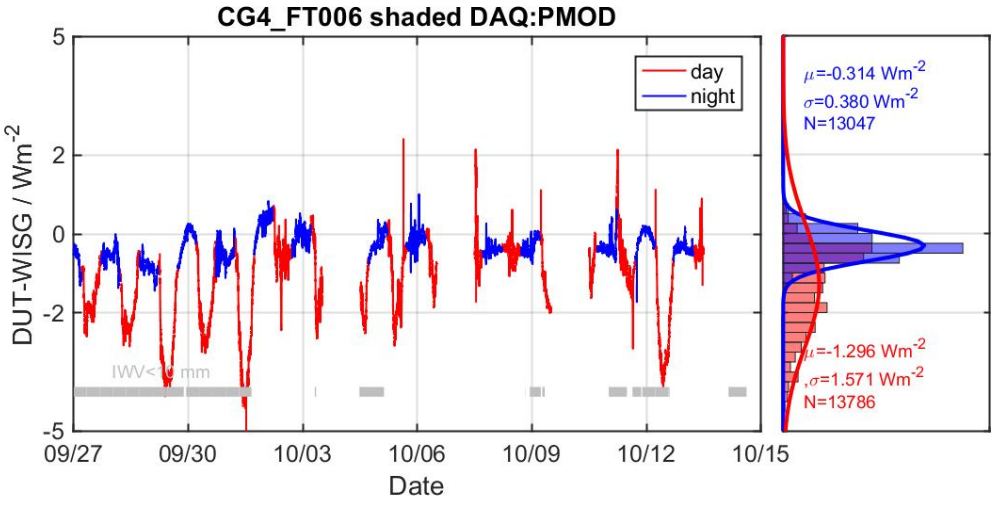
CG4_FT006 shaded DAQ:PMOD
day
night
μ=-0.314 Wm-2
σ=0.380 Wm-2
N=13047
μ=-1.296 Wm-2
σ=1.571 Wm-2
N=13786
DUT-WISG / Wm-2
Date
09/27
09/30
10/03
10/06
10/09
10/12
10/15

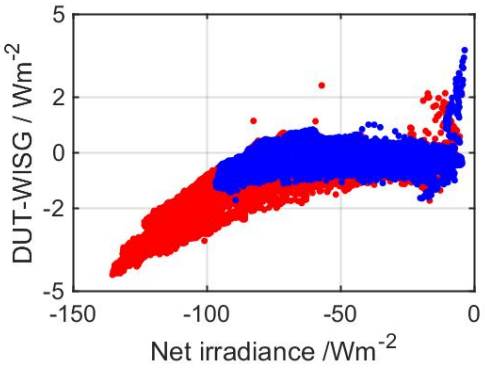
DUT-WISG / Wm-2
Net irradiance /Wm-2

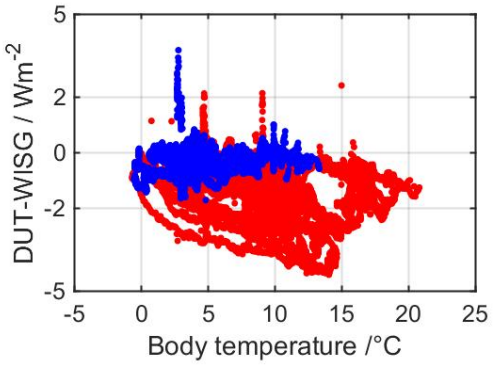
DUT-WISG / Wm-2
Body temperature /°C

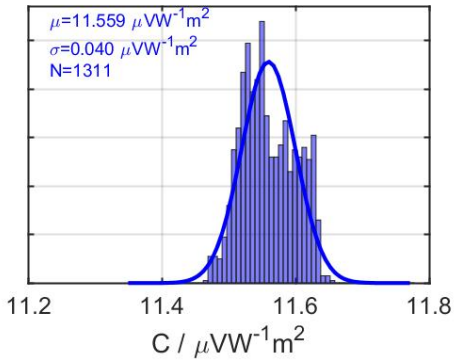
μ=11.559 μVW-1m2
σ=0.040 μVW-1m2
N=1311
C / μVW-1m2

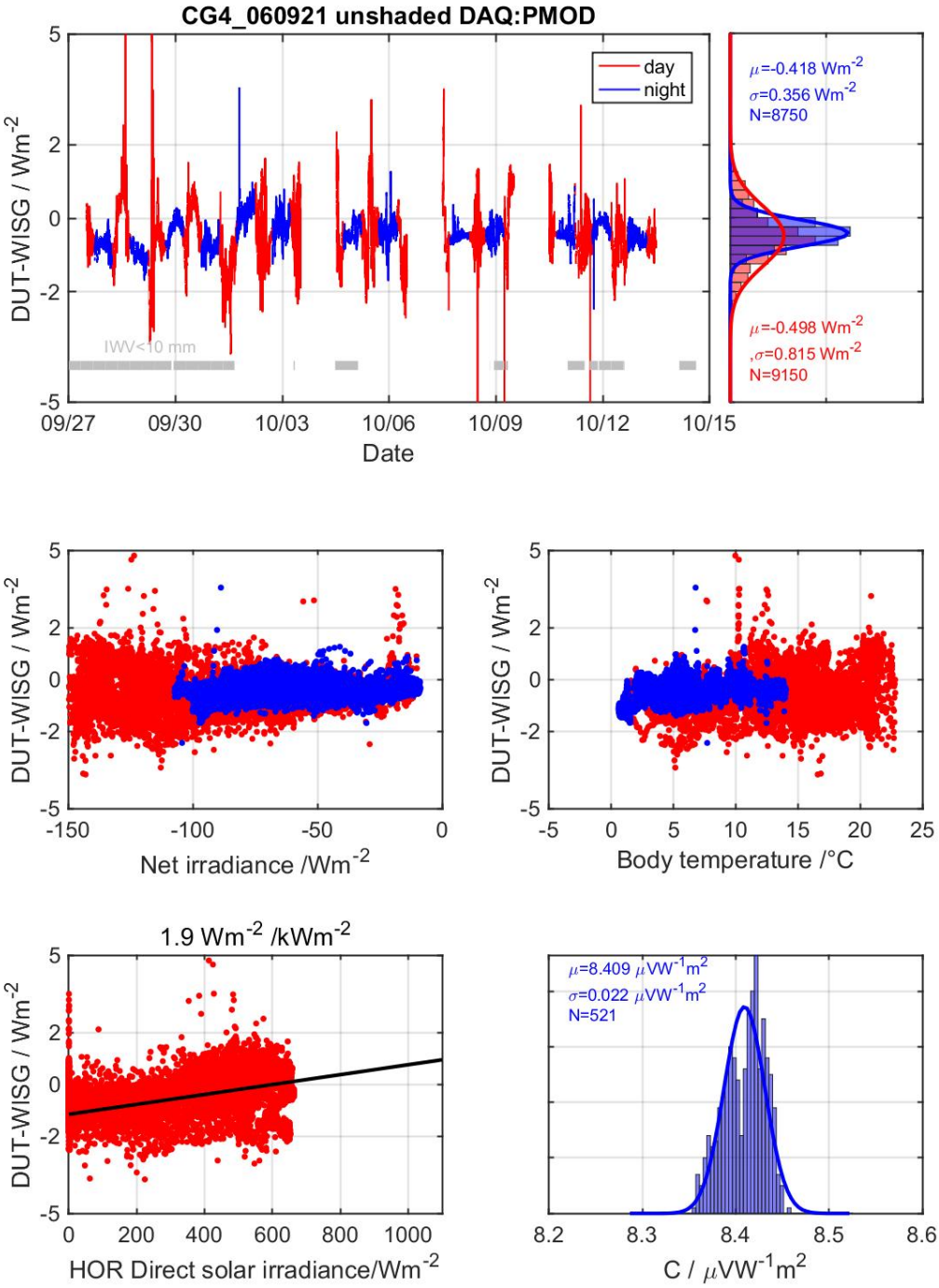
CG4_060921 unshaded DAQ:PMOD
day
night
μ=-0.418 Wm-2
σ=0.356 Wm-2
N=8750
μ=-0.498 Wm-2
,σ=0.815 Wm-2
N=9150
IWV<10 mm
DUT-WISG / Wm-2
Date
09/27
09/30
10/03
10/06
10/09
10/12
10/15
Net irradiance /Wm-2
Body temperature /°C
1.9 Wm-2 /kWm-2
HOR Direct solar irradiance/Wm-2
μ=8.409 μVW-1m2
σ=0.022 μVW-1m2
N=521
C / μVW-1m2

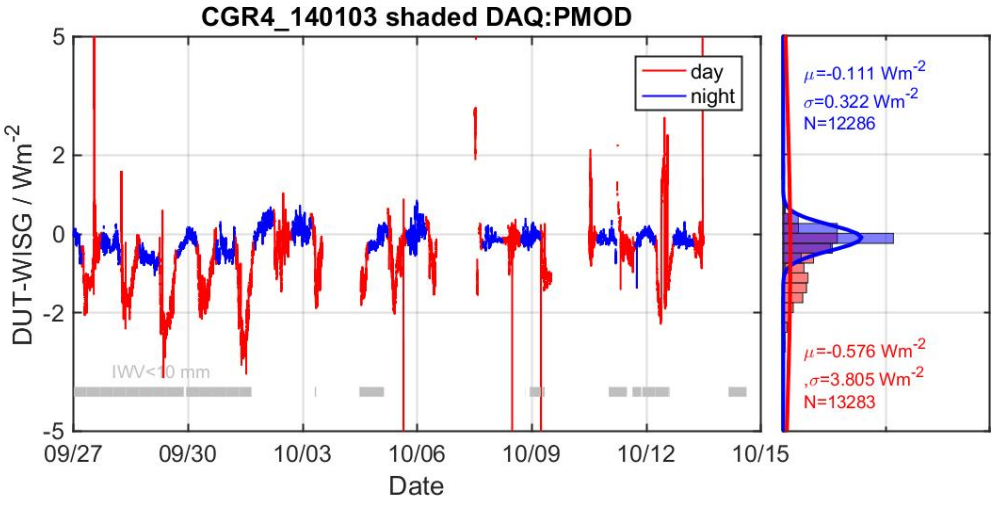
CGR4_140103 shaded DAQ:PMOD
DUT-WISG / Wm-2
day
night
IWV< 10 mm
μ=-0.111 Wm-2
σ=0.322 Wm-2
N=12286
μ=-0.576 Wm-2
,σ=3.805 Wm-2
N=13283
09/27
09/30
10/03
10/06
10/09
10/12
10/15
Date

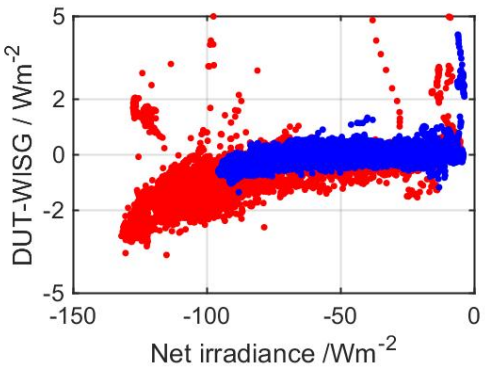
DUT-WISG / Wm-2
Net irradiance /Wm-2

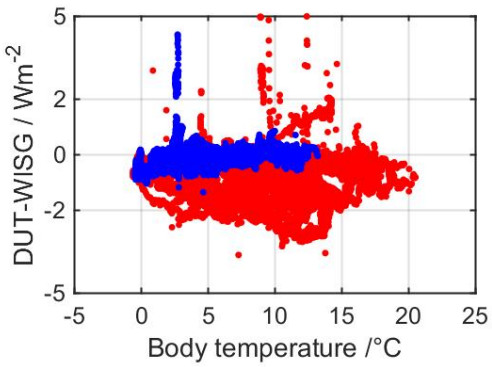
DUT-WISG / Wm-2
Body temperature /°C

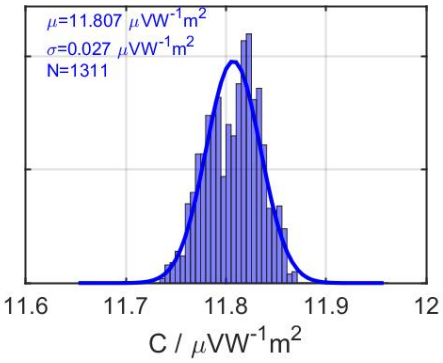
μ=11.807 μVW-1m2
σ=0.027 μVW-1m2
N=1311
C / μVW-1m2

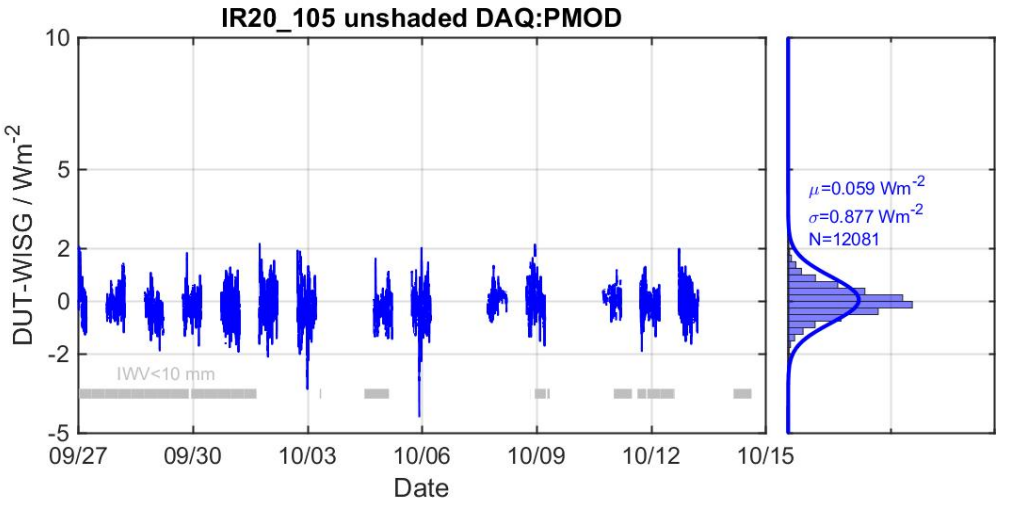
IR20_105 unshaded DAQ:PMOD
DUT-WISG / Wm-2
10
5
2
0
-2
-5
IWV<10 mm
09/27
09/30
10/03
10/06
10/09
10/12
10/15
Date
μ=0.059 Wm-2
σ=0.877 Wm-2
N=12081

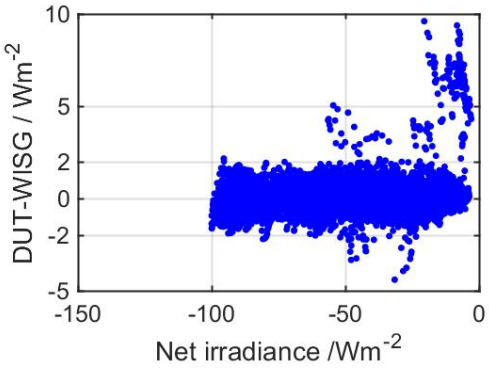
DUT-WISG / Wm-2
10
5
2
0
-2
-5
-150
-100
-50
0
Net irradiance /Wm-2

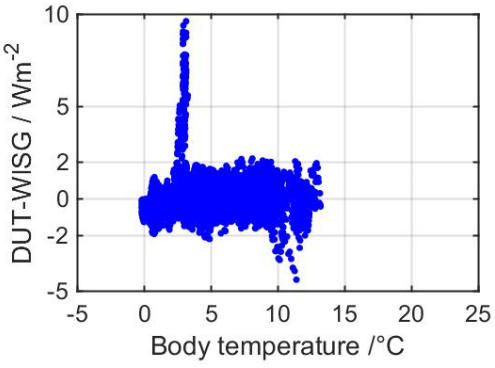
DUT-WISG / Wm-2
10
5
2
0
-2
-5
-5
0
5
10
15
20
25
Body temperature /°C

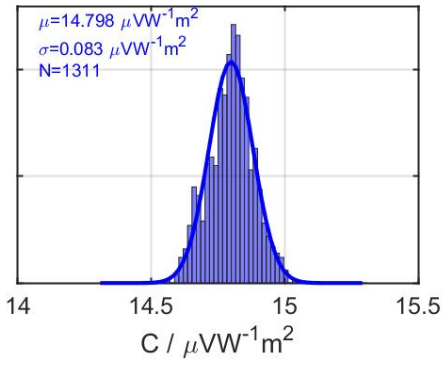
μ=14.798 μVW-1m2
σ=0.083 μVW-1m2
N=1311
14
14.5
15
15.5
C / μVW-1m2

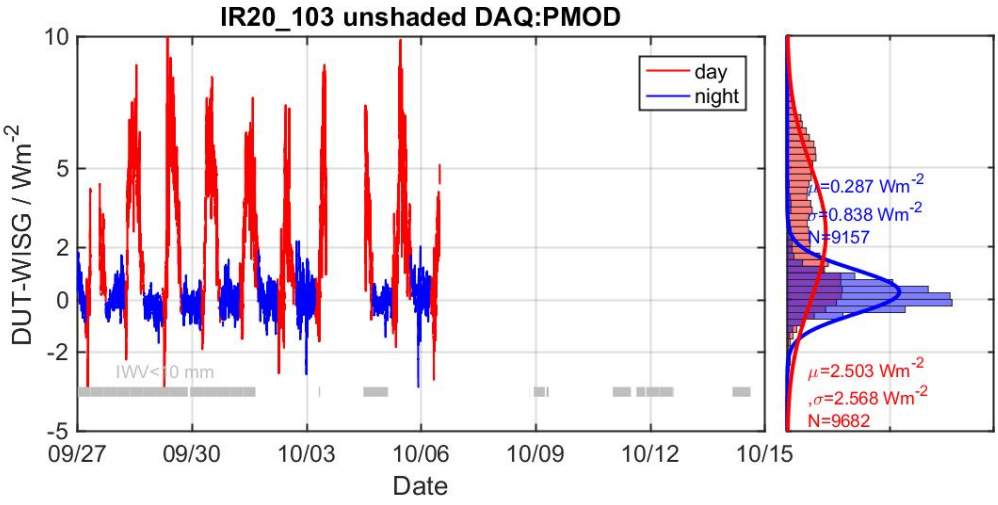
IR20_103 unshaded DAQ:PMOD
DUT-WISG / Wm-2
day
night
IWV<10 mm
μ=0.287 Wm-2
σ=0.838 Wm-2
N=9157
μ=2.503 Wm-2
σ=2.568 Wm-2
N=9682
09/27
09/30
10/03
10/06
10/09
10/12
10/15
Date

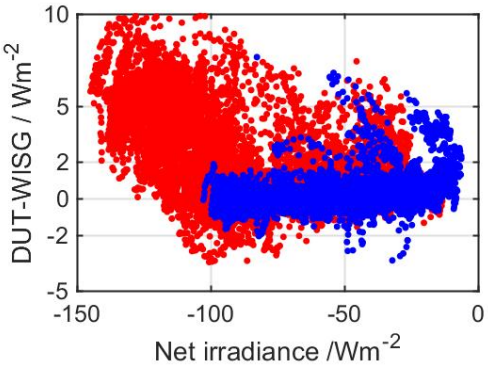
DUT-WISG / Wm-2
Net irradiance /Wm-2

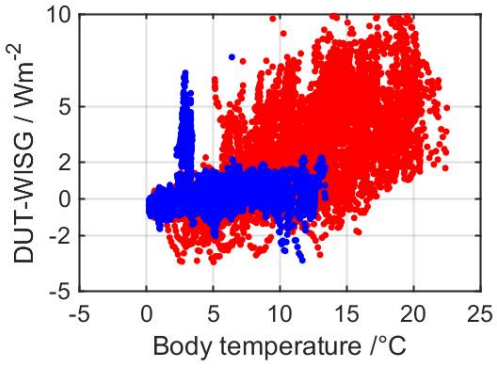
DUT-WISG / Wm-2
Body temperature /°C

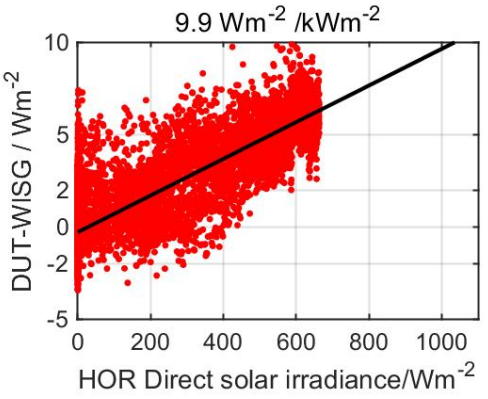
9.9 Wm-2 /kWm-2
DUT-WISG / Wm-2
HOR Direct solar irradiance/Wm-2

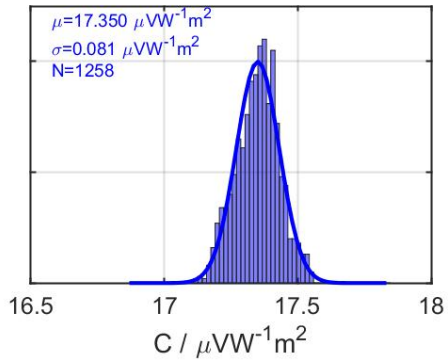
μ=17.350 μVW-1m2
σ=0.081 μVW-1m2
N=1258
C / μVW-1m2

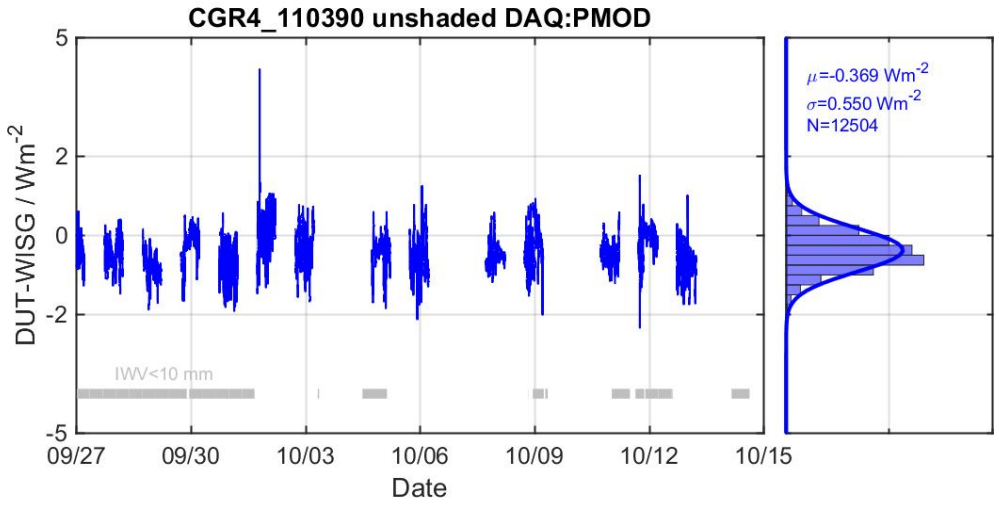
CGR4_110390 unshaded DAQ:PMOD
DUT-WISG / Wm-2
IWV<10 mm
09/27
09/30
10/03
10/06
10/09
10/12
10/15
Date
μ=-0.369 Wm-2
σ=0.550 Wm-2
N=12504

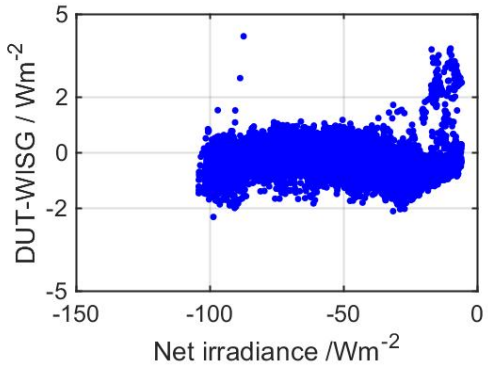
DUT-WISG / Wm-2
Net irradiance /Wm-2

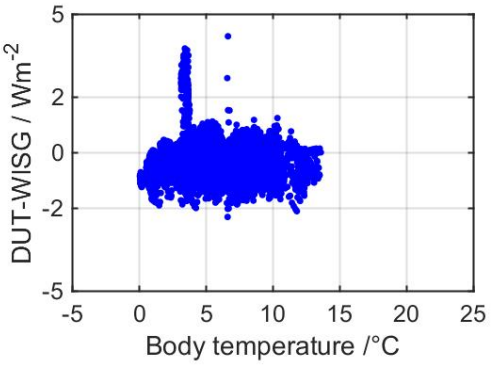
DUT-WISG / Wm-2
Body temperature /°C

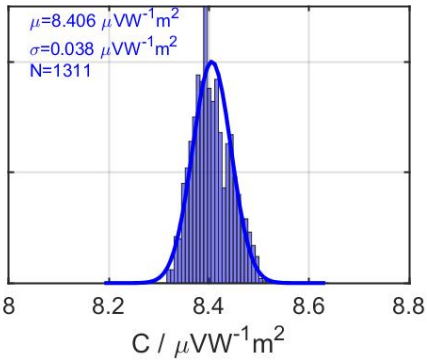
μ=8.406 μVW-1m2
σ=0.038 μVW-1m2
N=1311
C / μVW-1m2

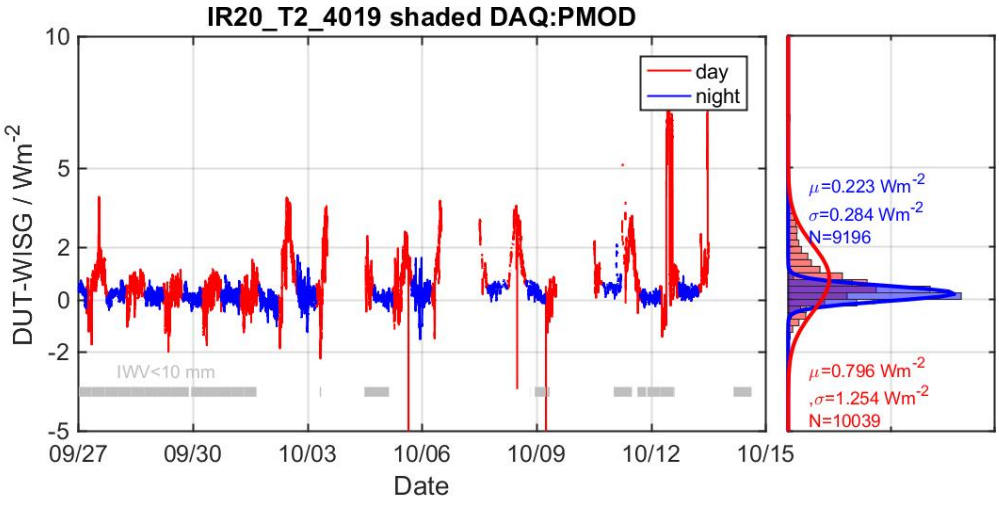
IR20_T2_4019 shaded DAQ:PMOD
day
night
IWV<10 mm
DUT-WISG / Wm-2
Date
09/27
09/30
10/03
10/06
10/09
10/12
10/15
μ=0.223 Wm-2
σ=0.284 Wm-2
N=9196
μ=0.796 Wm-2
,σ=1.254 Wm-2
N=10039

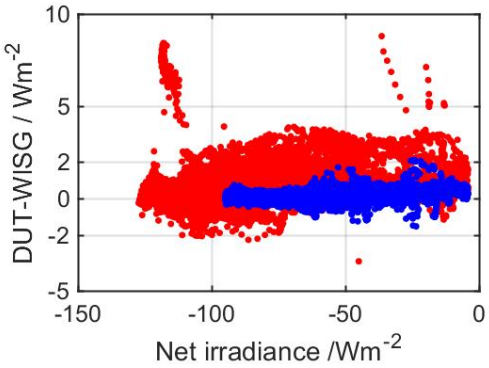
DUT-WISG / Wm-2
Net irradiance /Wm-2

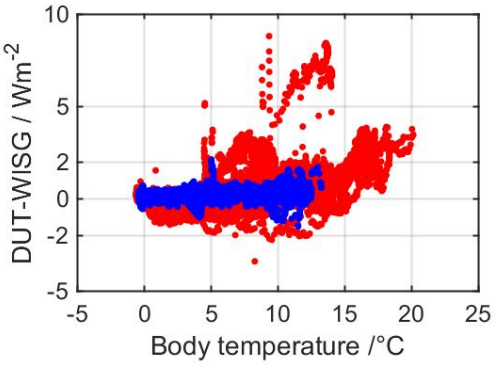
DUT-WISG / Wm-2
Body temperature /°C

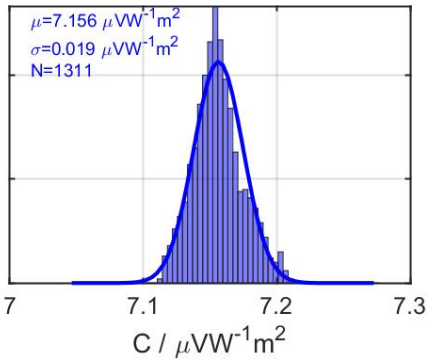
μ=7.156 μVW-1m2
σ=0.019 μVW-1m2
N=1311
C / μVW-1m2

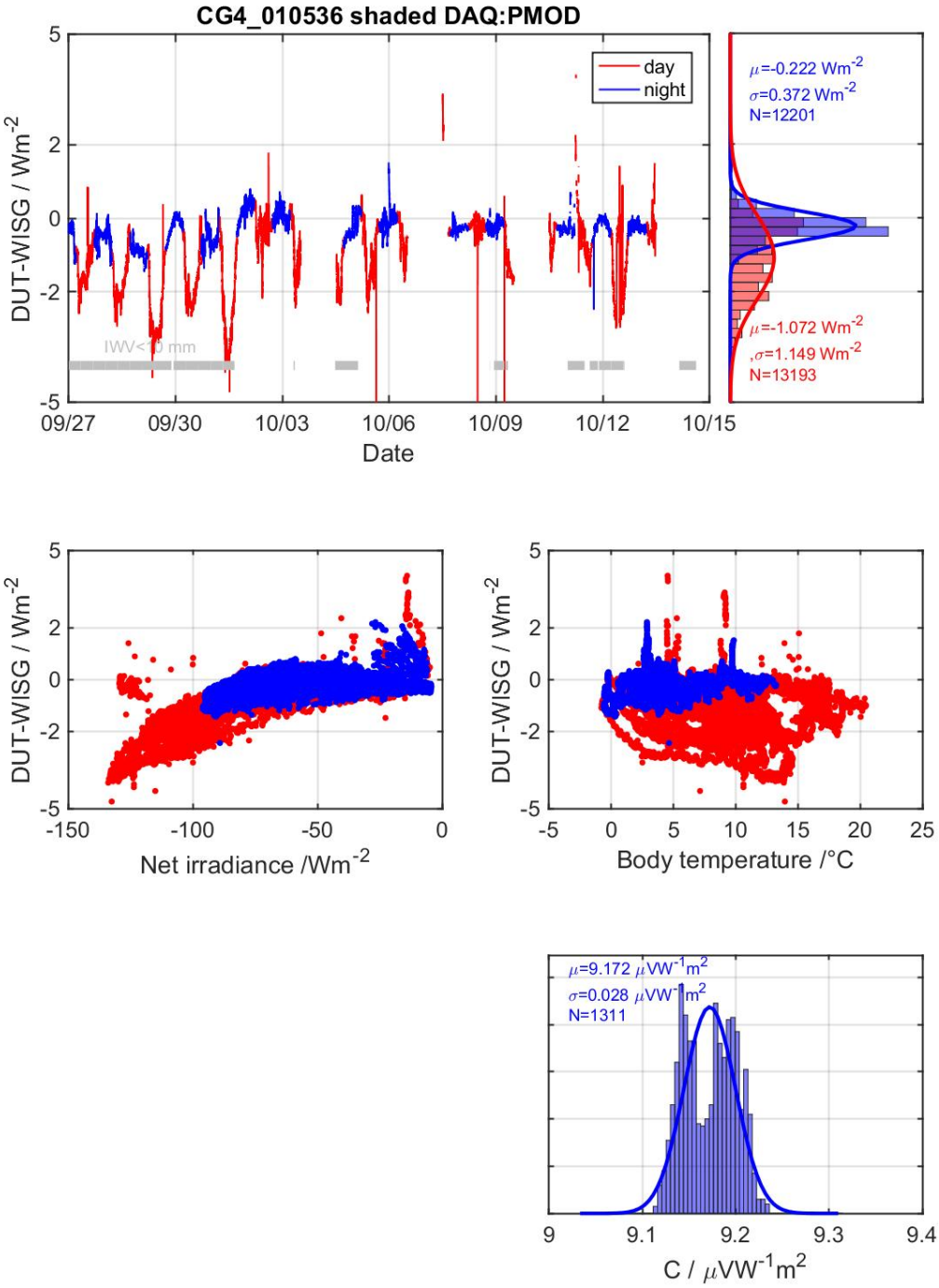
CG4_010536 shaded DAQ:PMOD
day
night
DUT-WISG / Wm-2
Date
09/27
09/30
10/03
10/06
10/09
10/12
10/15
μ=-0.222 Wm-2
σ=0.372 Wm-2
N=12201
μ=-1.072 Wm-2
,σ=1.149 Wm-2
N=13193
Net irradiance /Wm-2
Body temperature /°C
μ=9.172 μVW-1m2
σ=0.028 μVW-1m2
N=1311
C / μVW-1m2

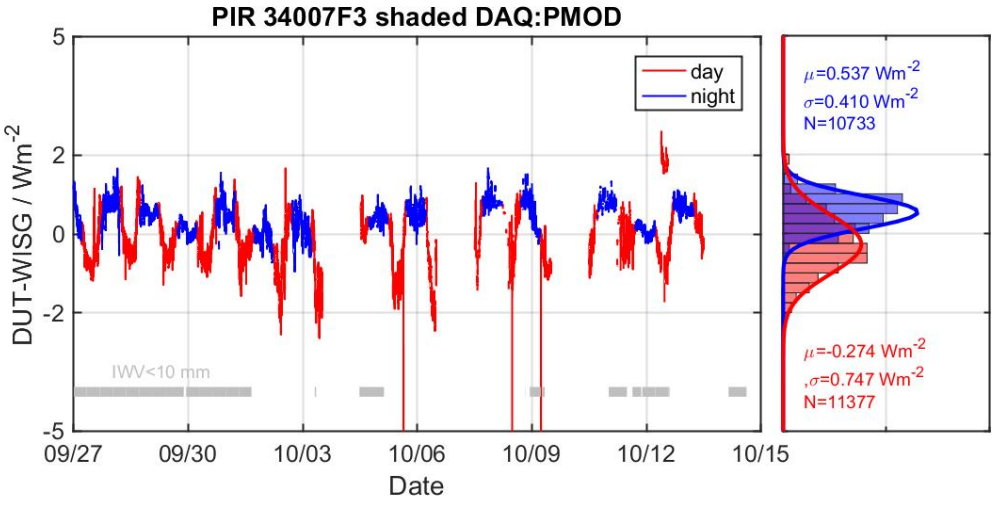
PIR 34007F3 shaded DAQ:PMOD
DUT-WISG / Wm-2
day
night
IWV<10 mm
μ=0.537 Wm-2
σ=0.410 Wm-2
N=10733
μ=-0.274 Wm-2
,σ=0.747 Wm-2
N=11377
09/27
09/30
10/03
10/06
10/09
10/12
10/15
Date

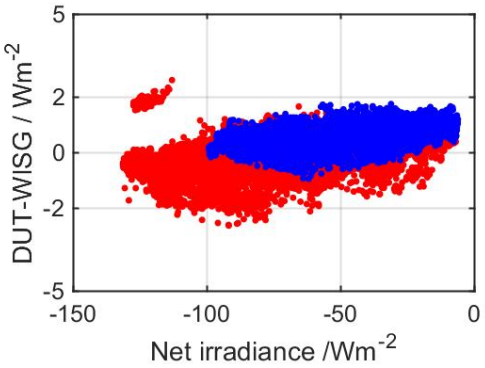
DUT-WISG / Wm-2
Net irradiance /Wm-2

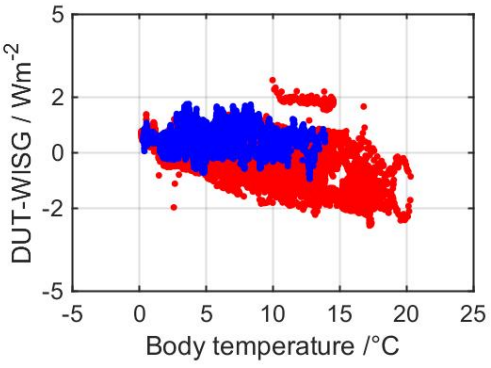
DUT-WISG / Wm-2
Body temperature /°C

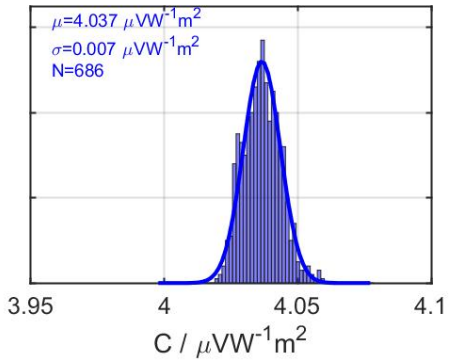
μ=4.037 μVW-1m2
σ=0.007 μVW-1m2
N=686
C / μVW-1m2

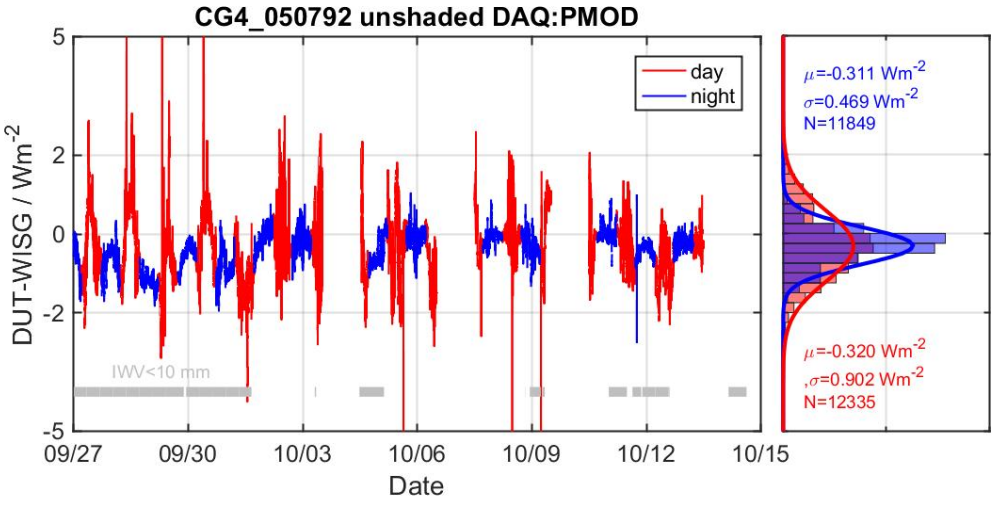
CG4_050792 unshaded DAQ:PMOD
day
night
IWV<10 mm
DUT-WISG / Wm-2
Date
09/27
09/30
10/03
10/06
10/09
10/12
10/15
μ=-0.311 Wm-2
σ=0.469 Wm-2
N=11849
μ=-0.320 Wm-2
,σ=0.902 Wm-2
N=12335

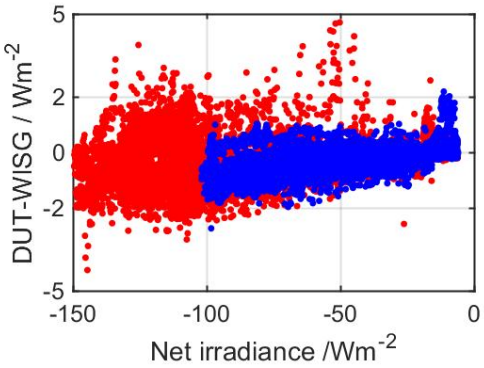
DUT-WISG / Wm-2
Net irradiance /Wm-2

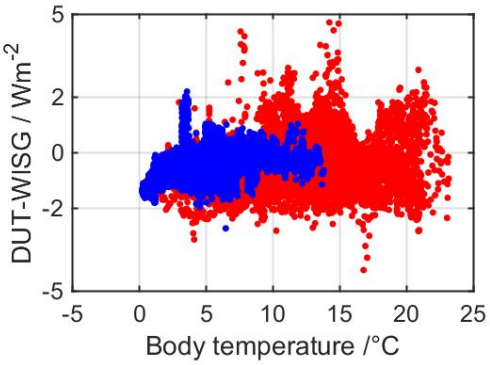
DUT-WISG / Wm-2
Body temperature /°C

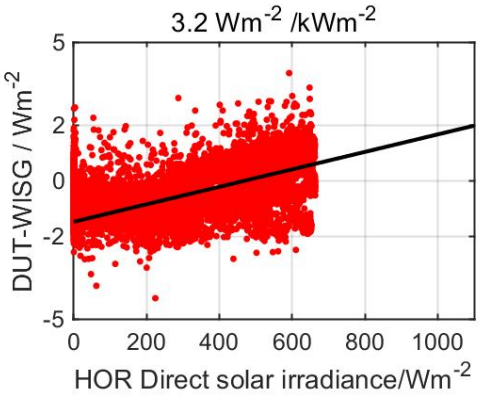
3.2 Wm-2 /kWm-2
DUT-WISG / Wm-2
HOR Direct solar irradiance/Wm-2

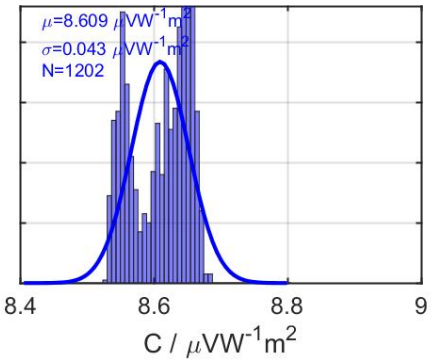
μ=8.609 μVW-1m2
σ=0.043 μVW-1m2
N=1202
C / μVW-1m2

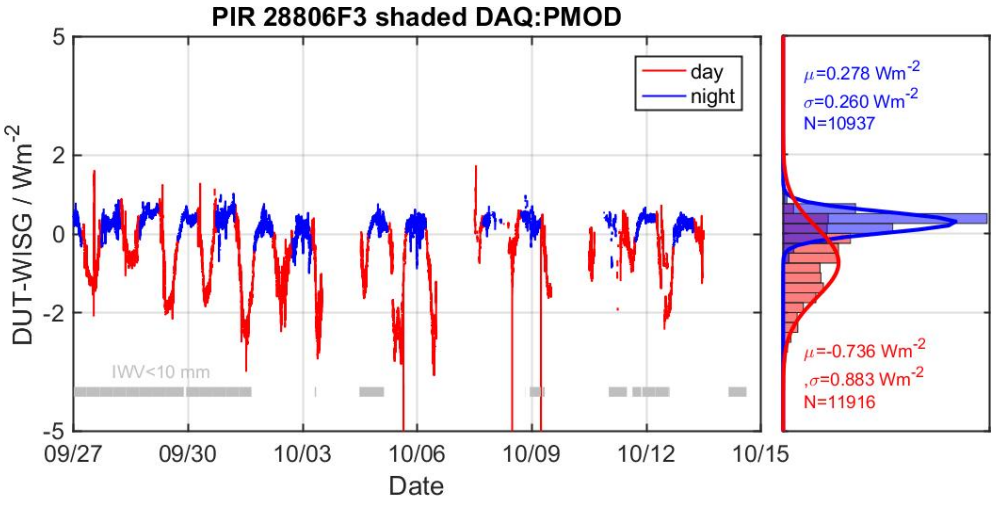
PIR 28806F3 shaded DAQ:PMOD
day
night
IWV<10 mm
DUT-WISG / Wm-2
Date
09/27
09/30
10/03
10/06
10/09
10/12
10/15
μ=0.278 Wm-2
σ=0.260 Wm-2
N=10937
μ=-0.736 Wm-2
,σ=0.883 Wm-2
N=11916

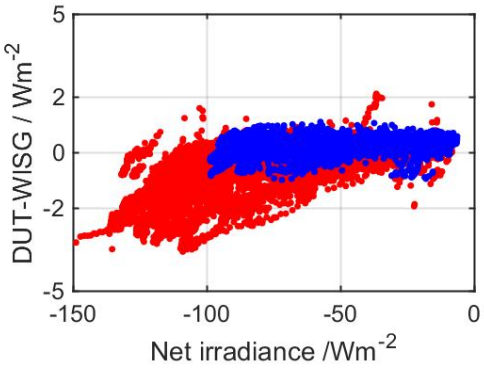
DUT-WISG / Wm-2
Net irradiance /Wm-2

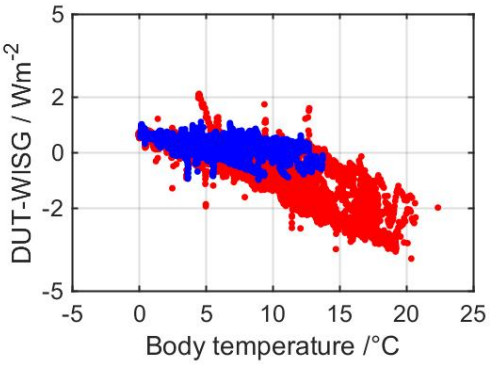
DUT-WISG / Wm-2
Body temperature /°C

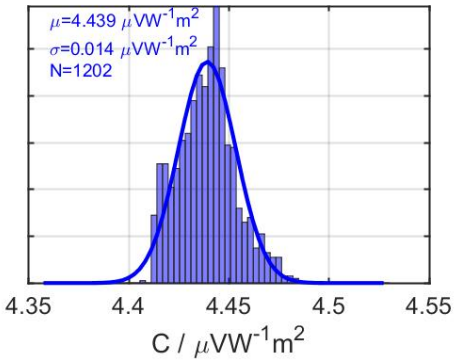
μ=4.439 μVW-1m2
σ=0.014 μVW-1m2
N=1202
C / μVW-1m2

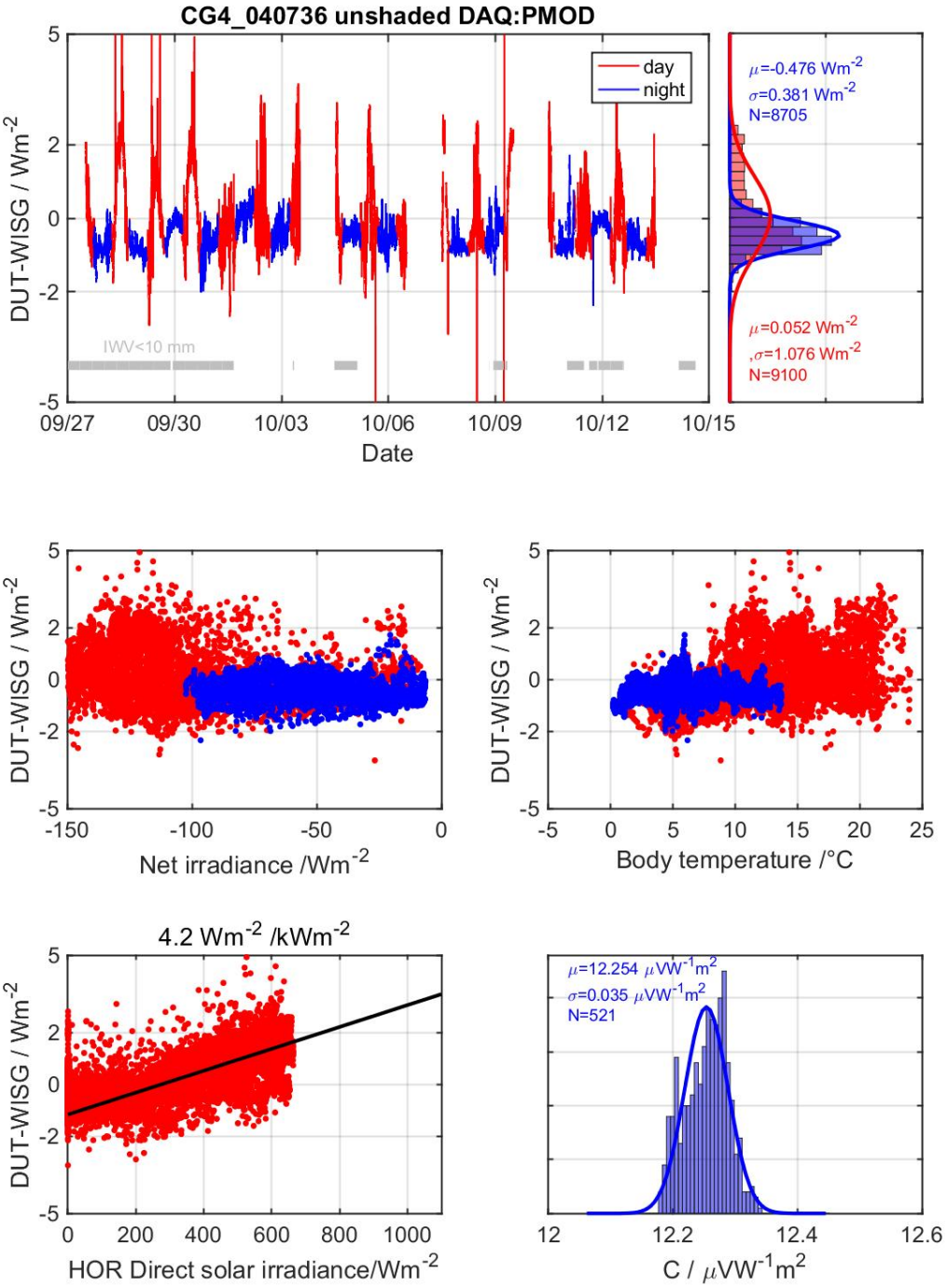
CG4_040736 unshaded DAQ:PMOD
day
night
IWV<10 mm
DUT-WISG / Wm-2
Date
09/27
09/30
10/03
10/06
10/09
10/12
10/15
μ=-0.476 Wm-2
σ=0.381 Wm-2
N=8705
μ=0.052 Wm-2
,σ=1.076 Wm-2
N=9100
Net irradiance /Wm-2
Body temperature /°C
4.2 Wm-2 /kWm-2
HOR Direct solar irradiance/Wm-2
μ=12.254 μVW-1m2
σ=0.035 μVW-1m2
N=521
C / μVW-1m2

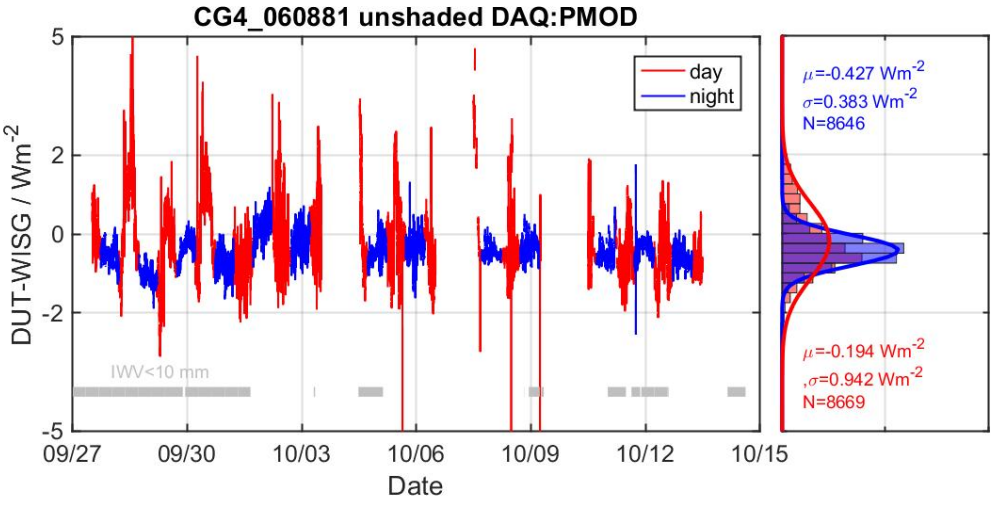
CG4_060881 unshaded DAQ:PMOD
day
night
IWV<10 mm
DUT-WISG / Wm-2
Date
09/27
09/30
10/03
10/06
10/09
10/12
10/15
μ=-0.427 Wm-2
σ=0.383 Wm-2
N=8646
μ=-0.194 Wm-2
,σ=0.942 Wm-2
N=8669

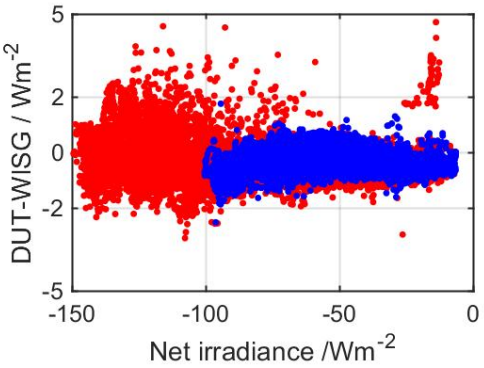
DUT-WISG / Wm-2
Net irradiance /Wm-2

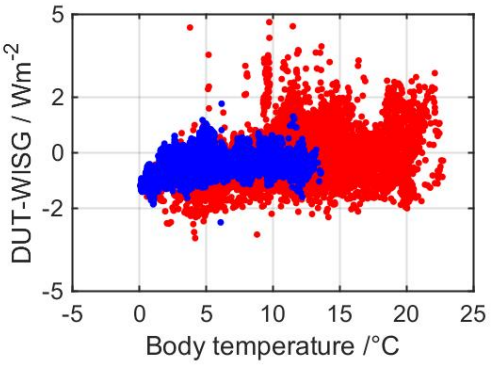
DUT-WISG / Wm-2
Body temperature /°C

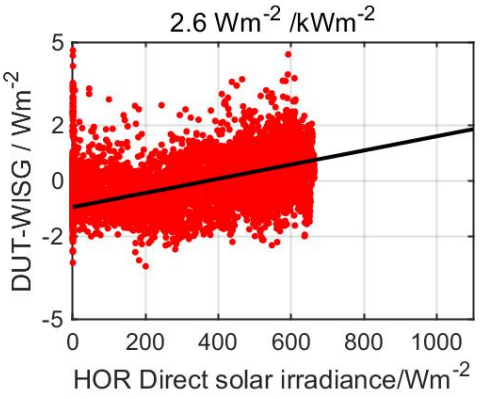
2.6 Wm-2 /kWm-2
DUT-WISG / Wm-2
HOR Direct solar irradiance/Wm-2

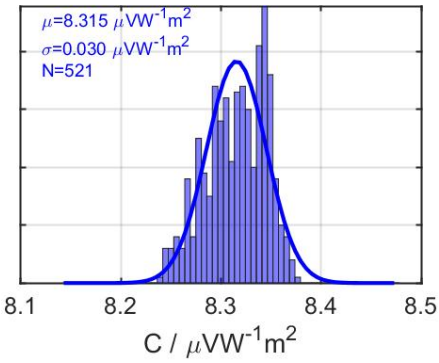
μ=8.315 μVW-1m2
σ=0.030 μVW-1m2
N=521
C / μVW-1m2

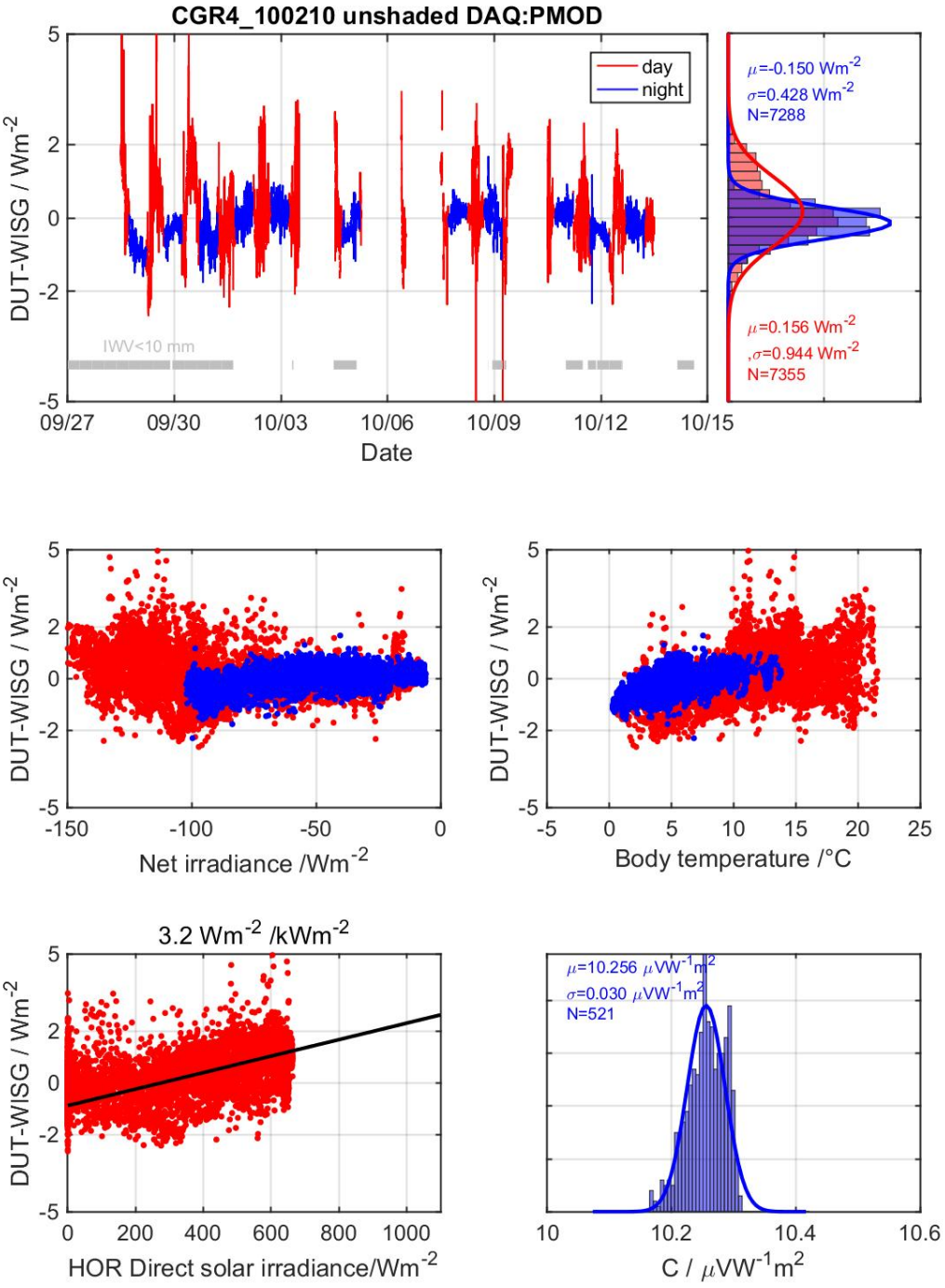
CGR4_100210 unshaded DAQ:PMOD
day
night
IWV<10 mm
DUT-WISG / Wm-2
Date
09/27
09/30
10/03
10/06
10/09
10/12
10/15
μ=-0.150 Wm-2
σ=0.428 Wm-2
N=7288
μ=0.156 Wm-2
,σ=0.944 Wm-2
N=7355
Net irradiance /Wm-2
Body temperature /°C
3.2 Wm-2 /kWm-2
HOR Direct solar irradiance/Wm-2
μ=10.256 μVW-1m2
σ=0.030 μVW-1m2
N=521
C / μVW-1m2

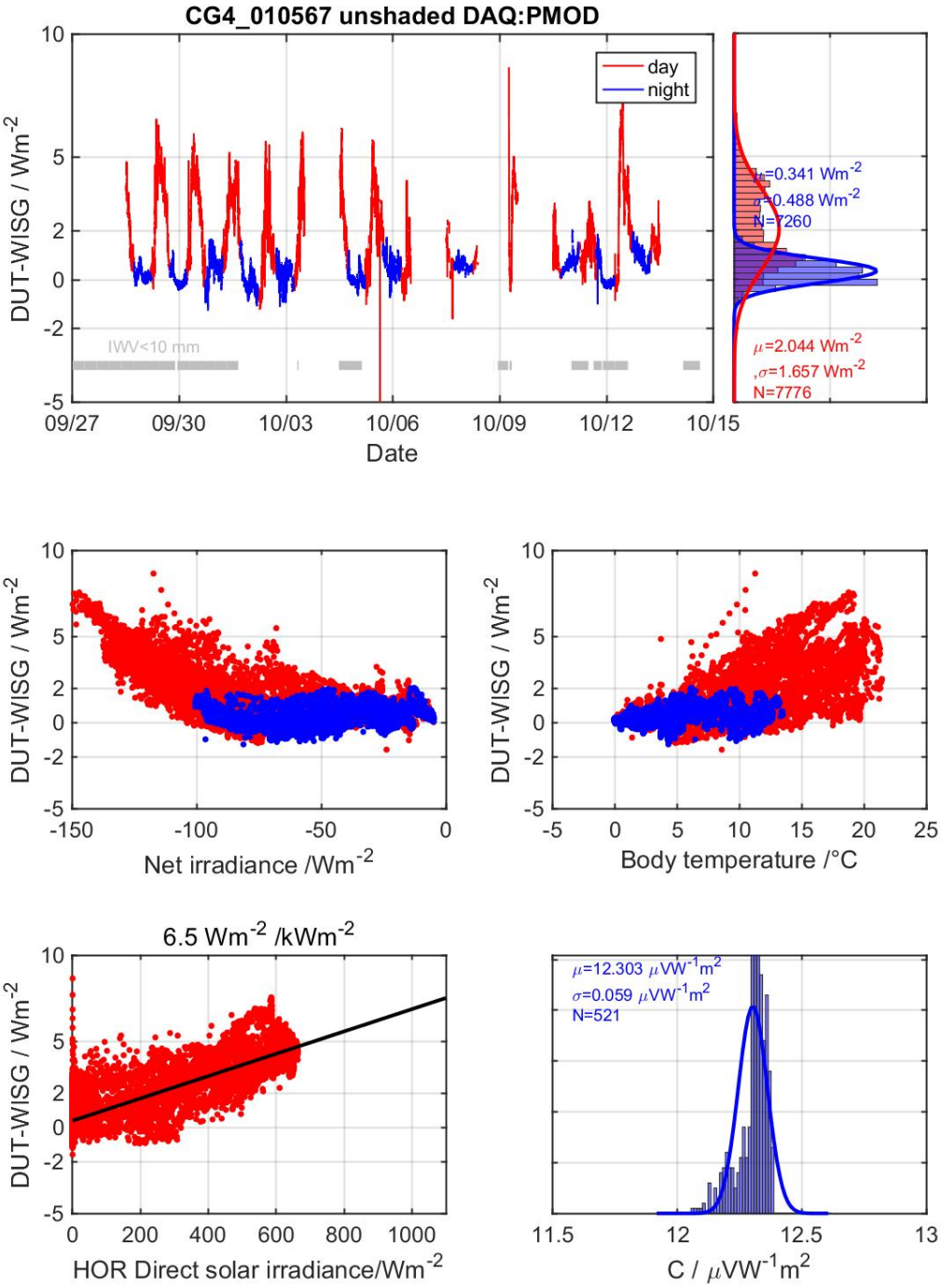
CG4_010567 unshaded DAQ:PMOD
day
night
DUT-WISG / Wm-2
IWV<10 mm
09/27
09/30
10/03
10/06
10/09
10/12
10/15
Date
μ=0.341 Wm-2
σ=0.488 Wm-2
N=7260
μ=2.044 Wm-2
,σ=1.657 Wm-2
N=7776
Net irradiance /Wm-2
Body temperature /°C
6.5 Wm-2 /kWm-2
HOR Direct solar irradiance/Wm-2
μ=12.303 μVW-1m2
σ=0.059 μVW-1m2
N=521
C / μVW-1m2

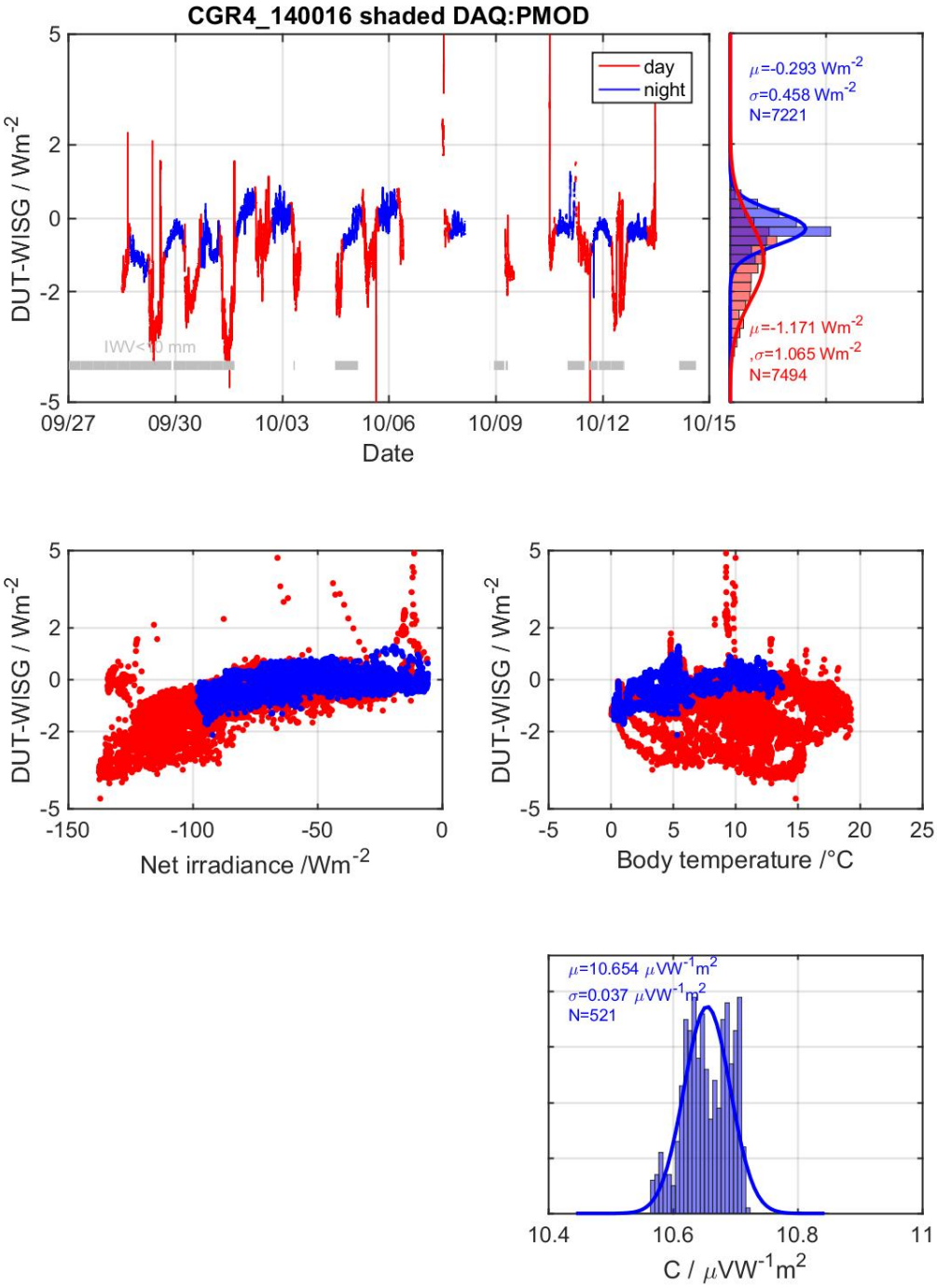
CGR4_140016 shaded DAQ:PMOD
day
night
μ=-0.293 Wm-2
σ=0.458 Wm-2
N=7221
μ=-1.171 Wm-2
,σ=1.065 Wm-2
N=7494
IWV<10 mm
DUT-WISG / Wm-2
Date
09/27
09/30
10/03
10/06
10/09
10/12
10/15
Net irradiance /Wm-2
Body temperature /°C
μ=10.654 μVW-1m2
σ=0.037 μVW-1m2
N=521
C / μVW-1m2

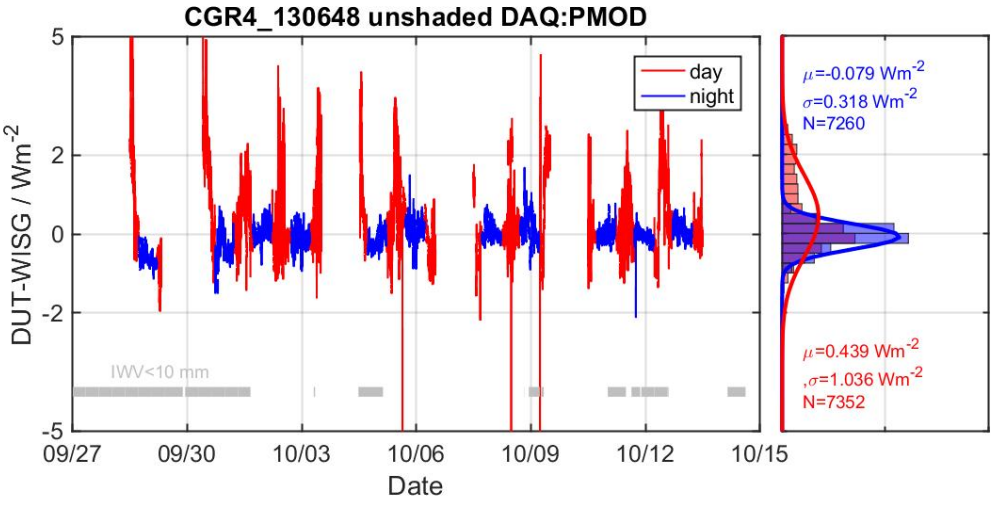
CGR4_130648 unshaded DAQ:PMOD
day
night
IWV<10 mm
DUT-WISG / Wm-2
Date
09/27
09/30
10/03
10/06
10/09
10/12
10/15
μ=-0.079 Wm-2
σ=0.318 Wm-2
N=7260
μ=0.439 Wm-2
,σ=1.036 Wm-2
N=7352

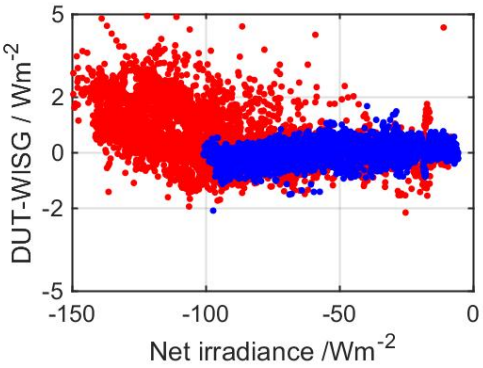
DUT-WISG / Wm-2
Net irradiance /Wm-2

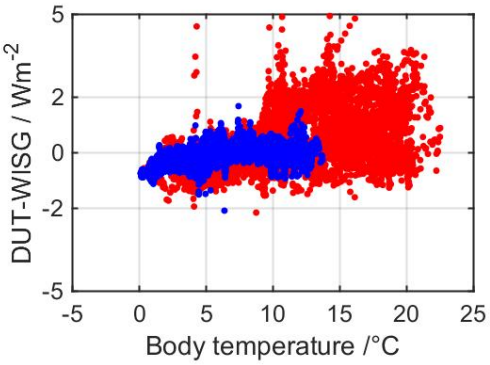
DUT-WISG / Wm-2
Body temperature /°C

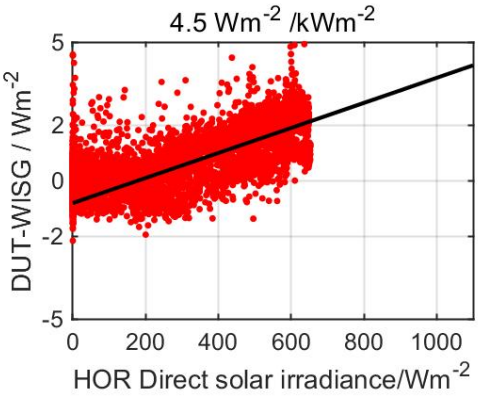
4.5 Wm-2 /kWm-2
DUT-WISG / Wm-2
HOR Direct solar irradiance/Wm-2

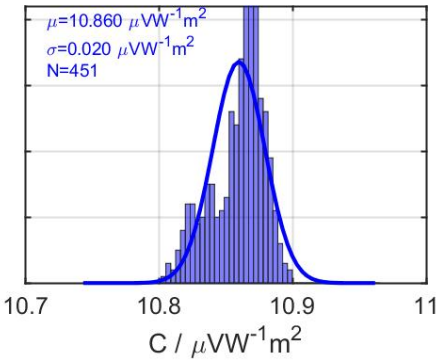
μ=10.860 μVW-1m2
σ=0.020 μVW-1m2
N=451
C / μVW-1m2

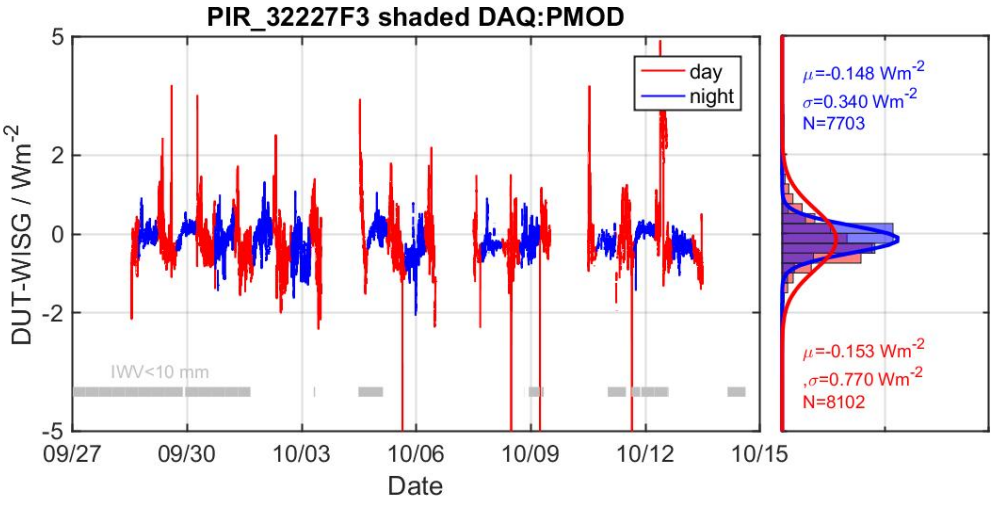
PIR_32227F3 shaded DAQ:PMOD
DUT-WISG / Wm-2
day
night
IWV<10 mm
μ=-0.148 Wm-2
σ=0.340 Wm-2
N=7703
μ=-0.153 Wm-2
,σ=0.770 Wm-2
N=8102
09/27
09/30
10/03
10/06
10/09
10/12
10/15
Date

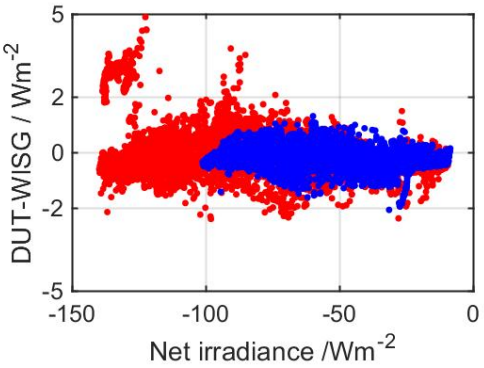
DUT-WISG / Wm-2
Net irradiance /Wm-2

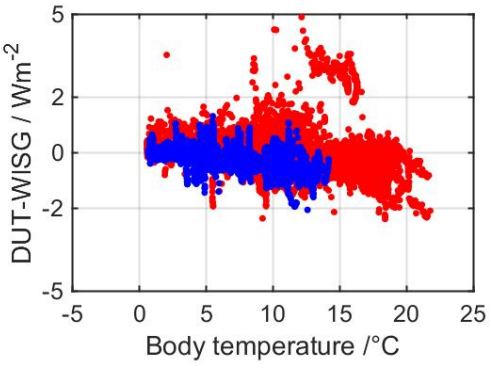
DUT-WISG / Wm-2
Body temperature /°C

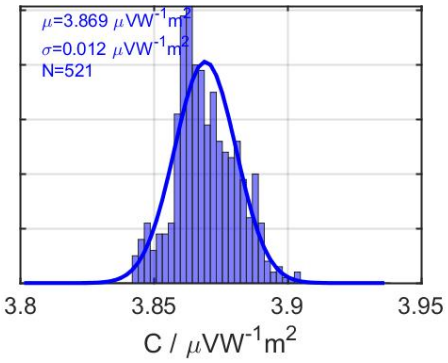
μ=3.869 μVW-1m2
σ=0.012 μVW-1m2
N=521
C / μVW-1m2

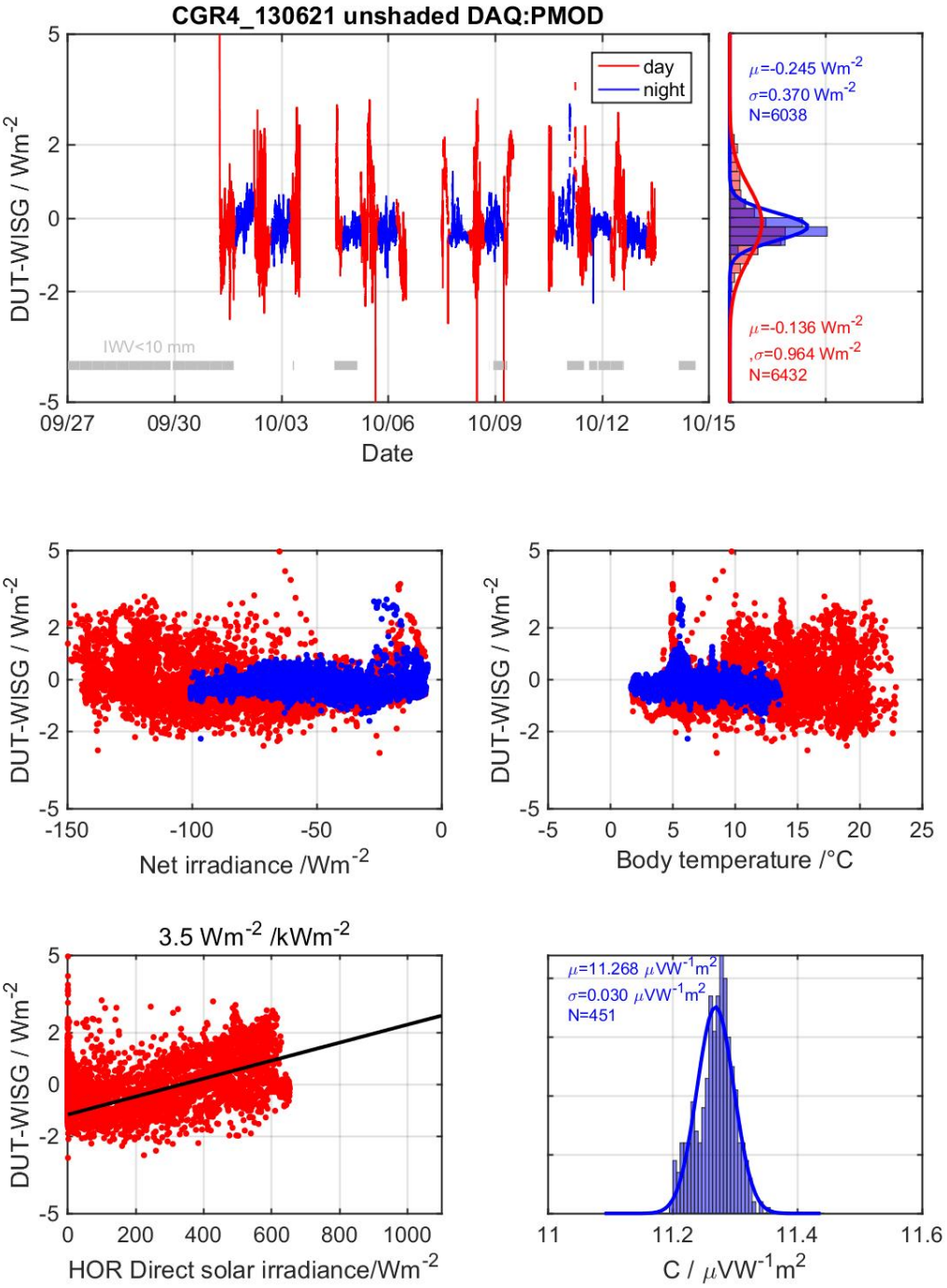
CGR4_130621 unshaded DAQ:PMOD
day
night
IWV<10 mm
DUT-WISG / Wm-2
Date
09/27
09/30
10/03
10/06
10/09
10/12
10/15
μ=-0.245 Wm-2
σ=0.370 Wm-2
N=6038
μ=-0.136 Wm-2
,σ=0.964 Wm-2
N=6432
Net irradiance /Wm-2
Body temperature /°C
3.5 Wm-2 /kWm-2
HOR Direct solar irradiance/Wm-2
μ=11.268 μVW-1m2
σ=0.030 μVW-1m2
N=451
C / μVW-1m2

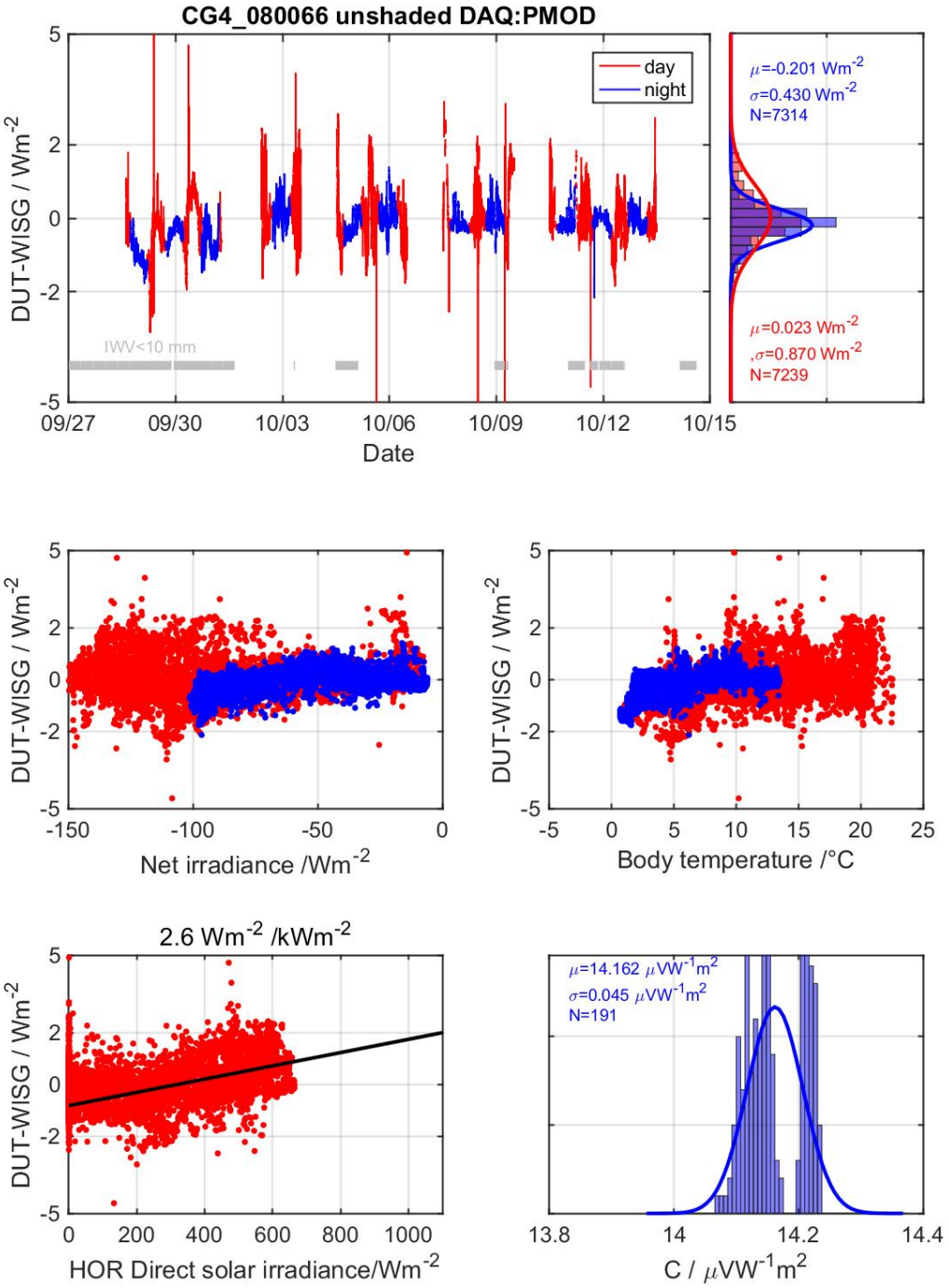
CG4_080066 unshaded DAQ:PMOD
day
night
IWV<10 mm
DUT-WISG / Wm-2
Date
09/27
09/30
10/03
10/06
10/09
10/12
10/15
μ=-0.201 Wm-2
σ=0.430 Wm-2
N=7314
μ=0.023 Wm-2
,σ=0.870 Wm-2
N=7239
Net irradiance /Wm-2
Body temperature /°C
2.6 Wm-2 /kWm-2
HOR Direct solar irradiance/Wm-2
μ=14.162 μVW-1m2
σ=0.045 μVW-1m2
N=191
C / μVW-1m2

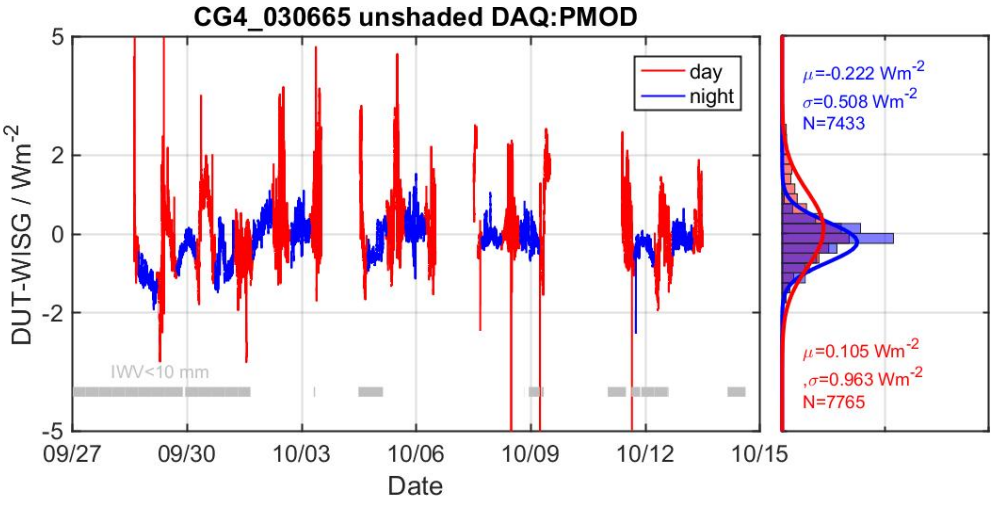
CG4_030665 unshaded DAQ:PMOD
day
night
IWV<10 mm
DUT-WISG / Wm-2
Date
09/27
09/30
10/03
10/06
10/09
10/12
10/15
μ=-0.222 Wm-2
σ=0.508 Wm-2
N=7433
μ=0.105 Wm-2
,σ=0.963 Wm-2
N=7765

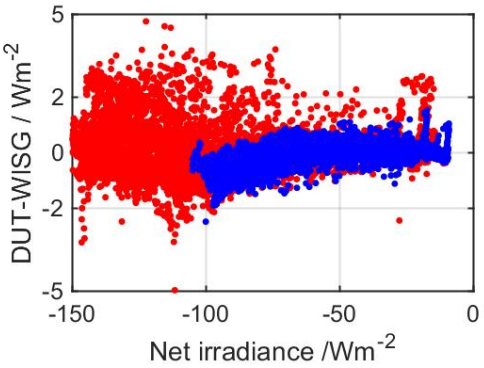
DUT-WISG / Wm-2
Net irradiance /Wm-2

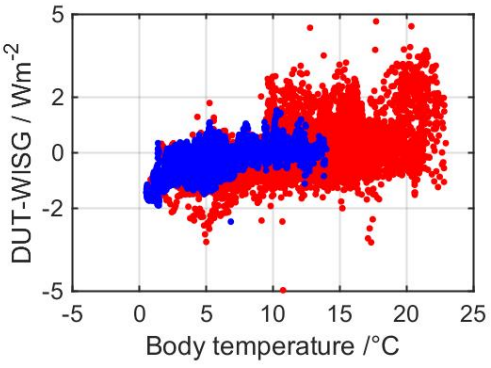
DUT-WISG / Wm-2
Body temperature /°C

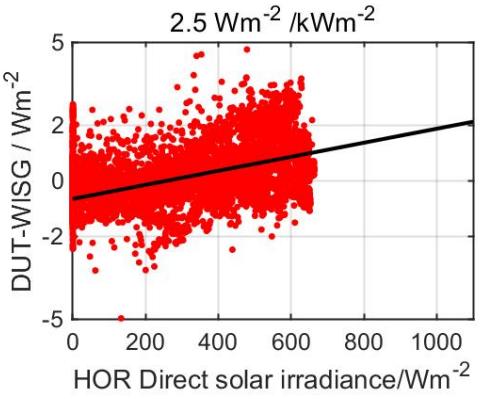
2.5 Wm-2 /kWm-2
DUT-WISG / Wm-2
HOR Direct solar irradiance/Wm-2

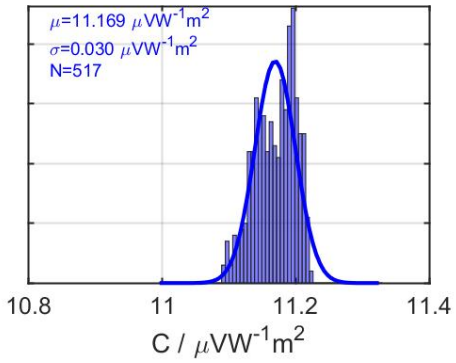
μ=11.169 μVW-1m2
σ=0.030 μVW-1m2
N=517
C / μVW-1m2

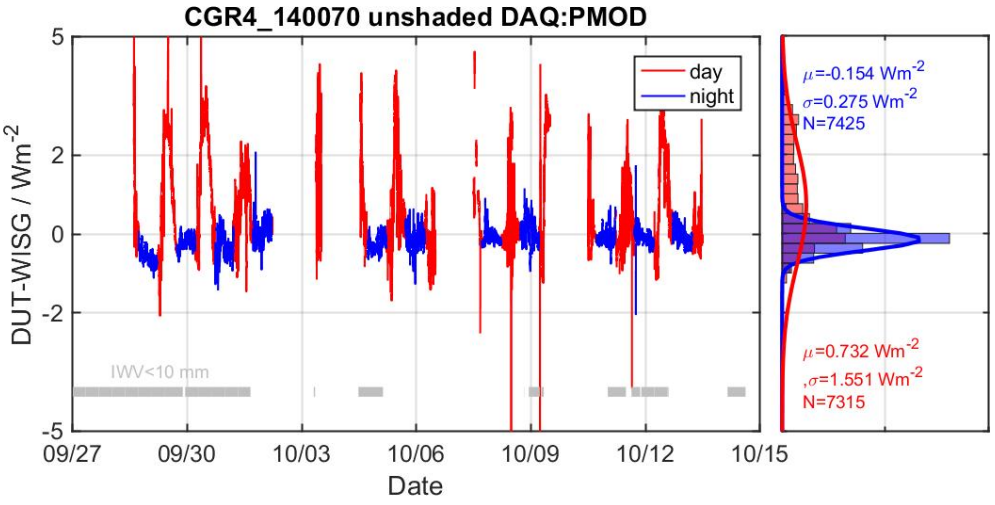
CGR4_140070 unshaded DAQ:PMOD
DUT-WISG / Wm-2
day
night
IWV<10 mm
μ=-0.154 Wm-2
σ=0.275 Wm-2
N=7425
μ=0.732 Wm-2
,σ=1.551 Wm-2
N=7315
09/27
09/30
10/03
10/06
10/09
10/12
10/15
Date

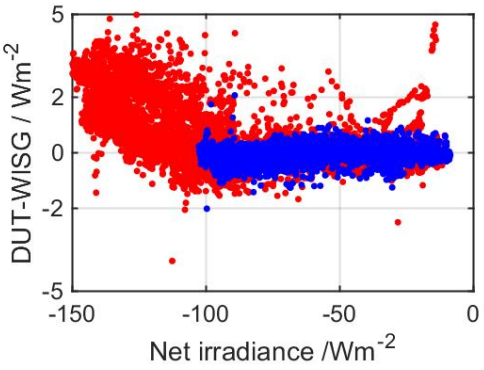
DUT-WISG / Wm-2
Net irradiance /Wm-2

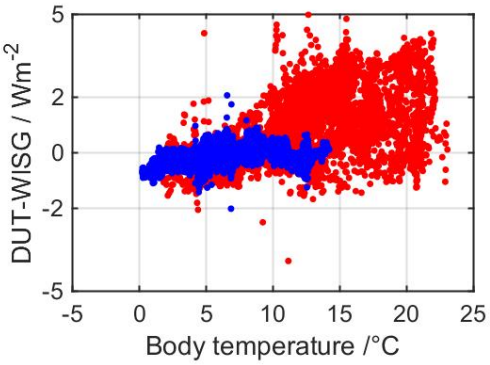
DUT-WISG / Wm-2
Body temperature /°C

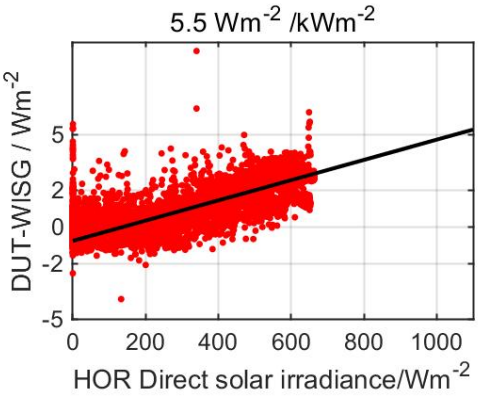
5.5 Wm-2 /kWm-2
DUT-WISG / Wm-2
HOR Direct solar irradiance/Wm-2

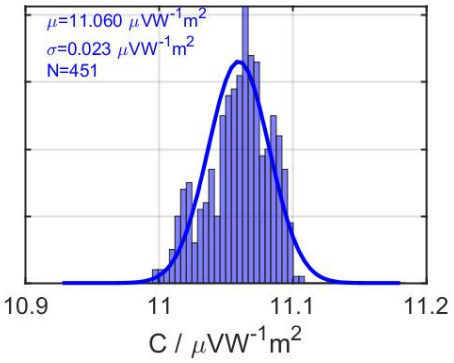
μ=11.060 μVW-1m2
σ=0.023 μVW-1m2
N=451
C / μVW-1m2

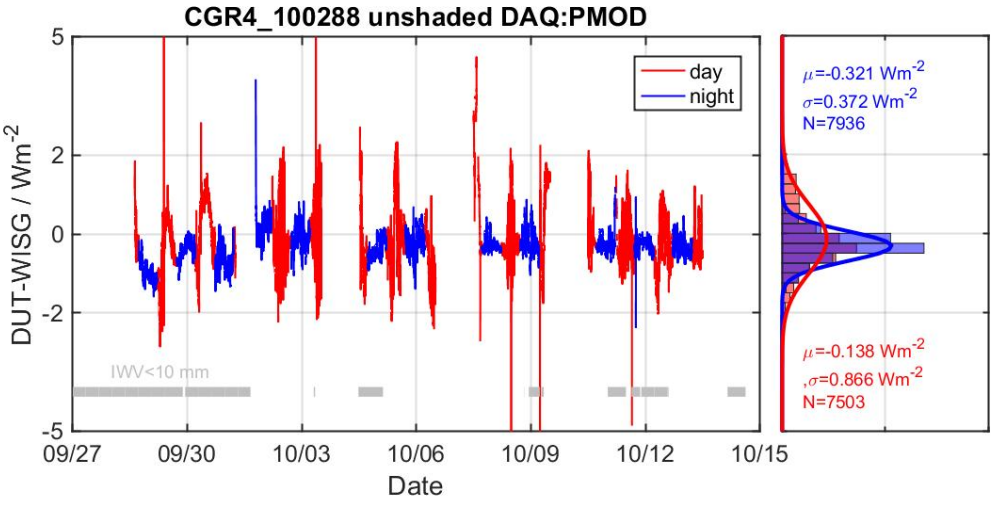
CGR4_100288 unshaded DAQ:PMOD
day
night
IWV<10 mm
DUT-WISG / Wm-2
Date
09/27
09/30
10/03
10/06
10/09
10/12
10/15
μ=-0.321 Wm-2
σ=0.372 Wm-2
N=7936
μ=-0.138 Wm-2
,σ=0.866 Wm-2
N=7503

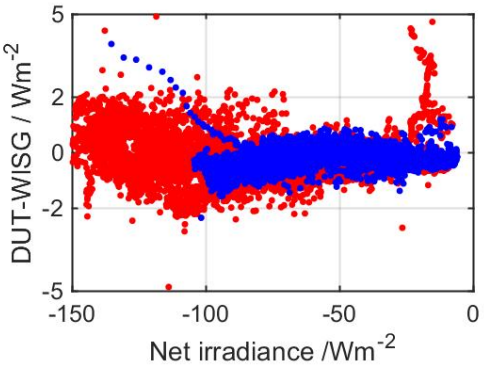
DUT-WISG / Wm-2
Net irradiance /Wm-2

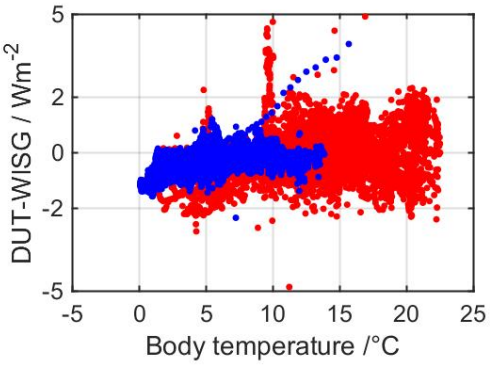
DUT-WISG / Wm-2
Body temperature /°C

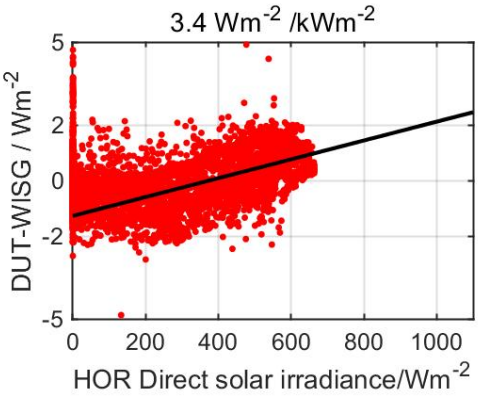
3.4 Wm-2 /kWm-2
DUT-WISG / Wm-2
HOR Direct solar irradiance/Wm-2

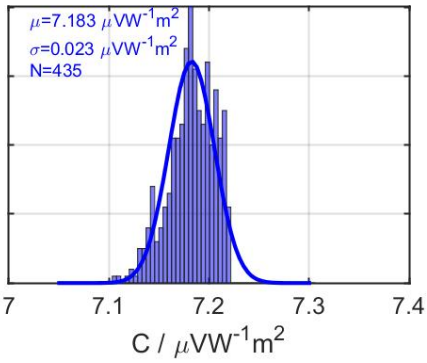
μ=7.183 μVW-1m2
σ=0.023 μVW-1m2
N=435
C / μVW-1m2

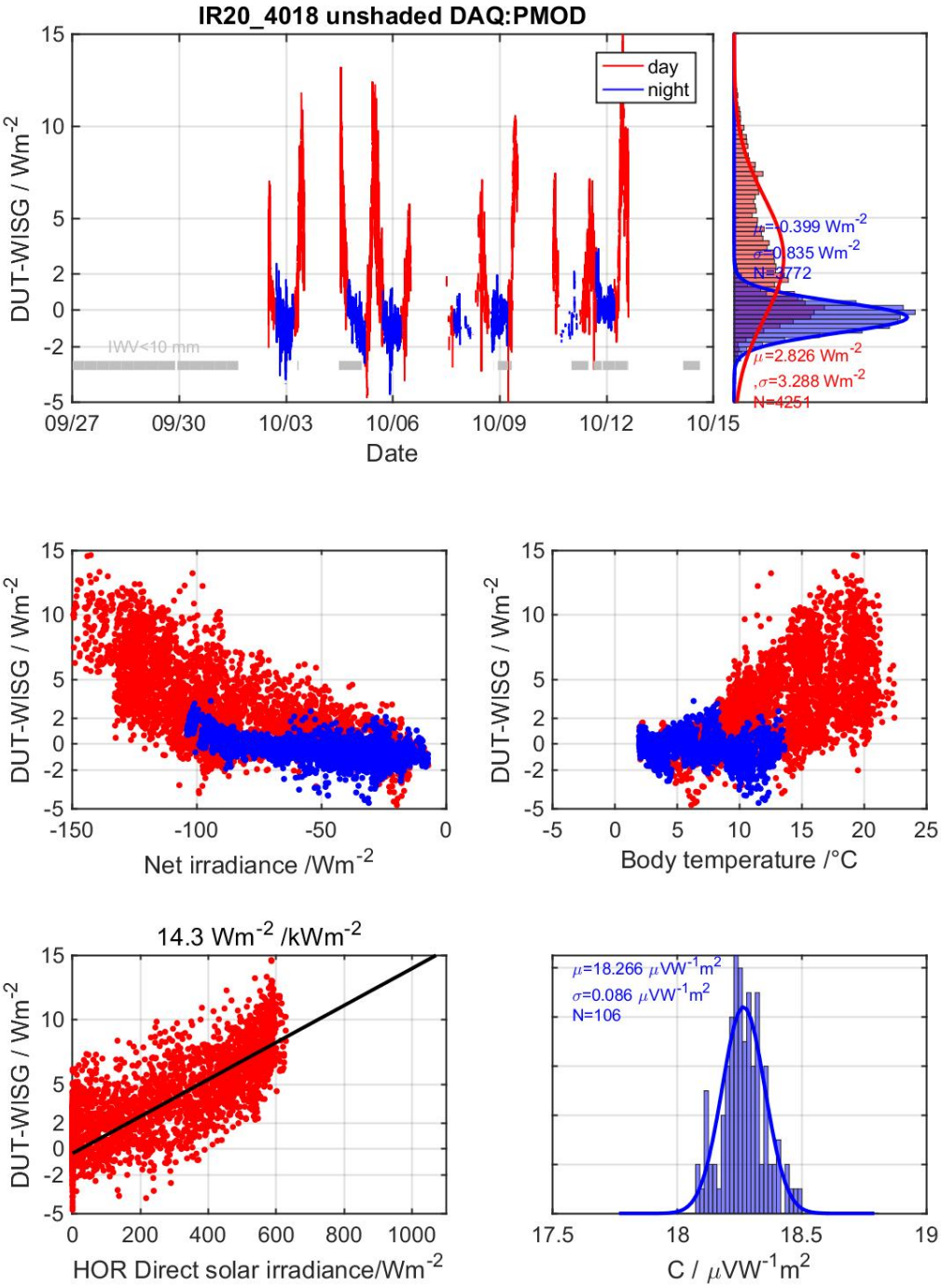
IR20_4018 unshaded DAQ:PMOD
day
night
DUT-WISG / Wm-2
IWV<10 mm
09/27
09/30
10/03
10/06
10/09
10/12
10/15
Date
μ=0.399 Wm-2
σ=0.835 Wm-2
N=3772
μ=2.826 Wm-2
σ=3.288 Wm-2
N=4251
Net irradiance /Wm-2
Body temperature /°C
14.3 Wm-2 /kWm-2
HOR Direct solar irradiance/Wm-2
μ=18.266 μVW-1m2
σ=0.086 μVW-1m2
N=106
C / μVW-1m2

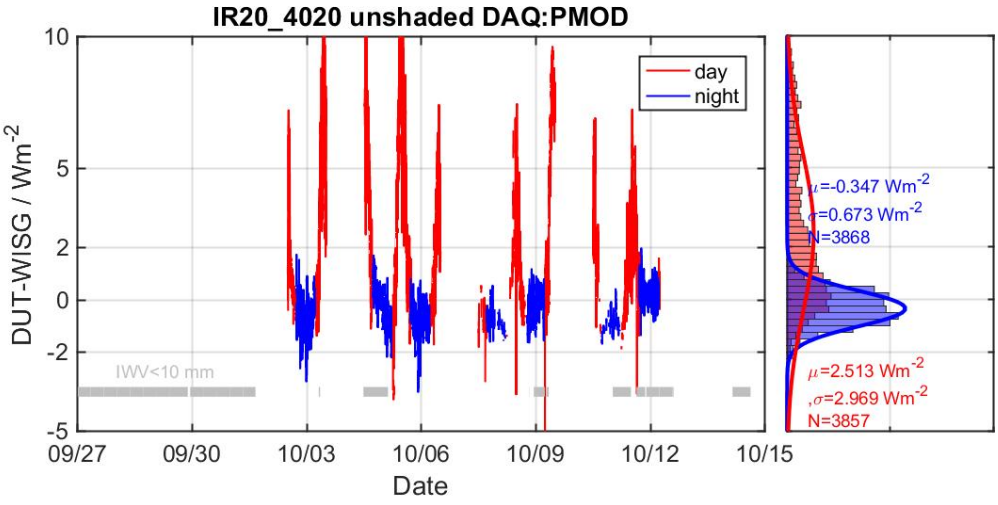
IR20_4020 unshaded DAQ:PMOD
DUT-WISG / Wm-2
day
night
IWV<10 mm
μ=-0.347 Wm-2
σ=0.673 Wm-2
N=3868
μ=2.513 Wm-2
,σ=2.969 Wm-2
N=3857
09/27
09/30
10/03
10/06
10/09
10/12
10/15
Date

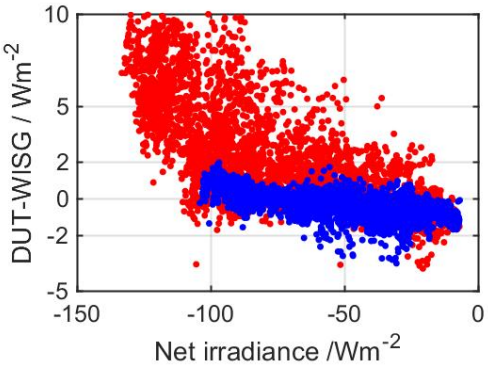
DUT-WISG / Wm-2
Net irradiance /Wm-2

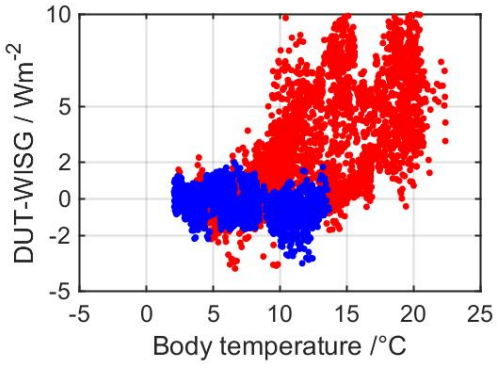
DUT-WISG / Wm-2
Body temperature /°C

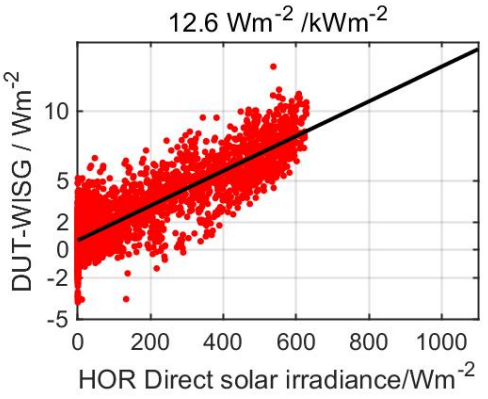
12.6 Wm-2 /kWm-2
DUT-WISG / Wm-2
HOR Direct solar irradiance/Wm-2

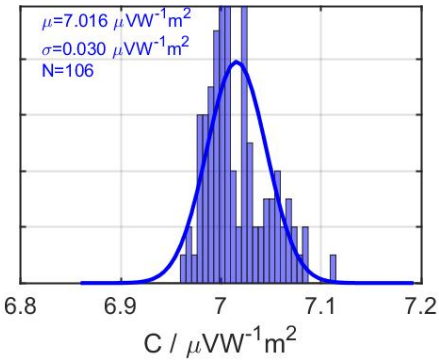
μ=7.016 μVW-1m2
σ=0.030 μVW-1m2
N=106
C / μVW-1m2

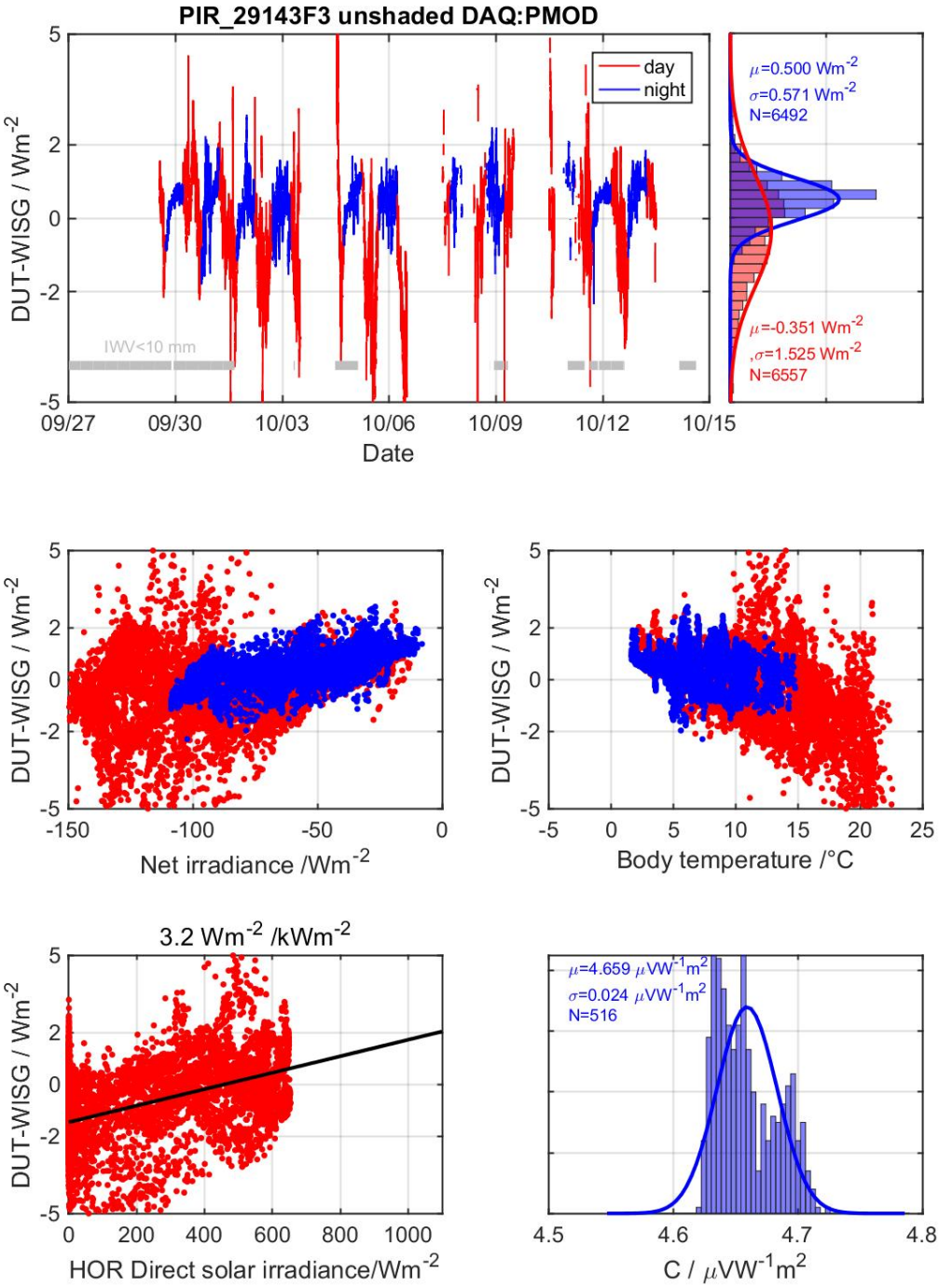
PIR_29143F3 unshaded DAQ:PMOD
DUT-WISG / Wm-2
day
night
IWV<10 mm
μ=0.500 Wm-2
σ=0.571 Wm-2
N=6492
μ=-0.351 Wm-2
,σ=1.525 Wm-2
N=6557
09/27
09/30
10/03
10/06
10/09
10/12
10/15
Date
Net irradiance /Wm-2
Body temperature /°C
3.2 Wm-2 /kWm-2
HOR Direct solar irradiance/Wm-2
μ=4.659 μVW-1m2
σ=0.024 μVW-1m2
N=516
C / μVW-1m2

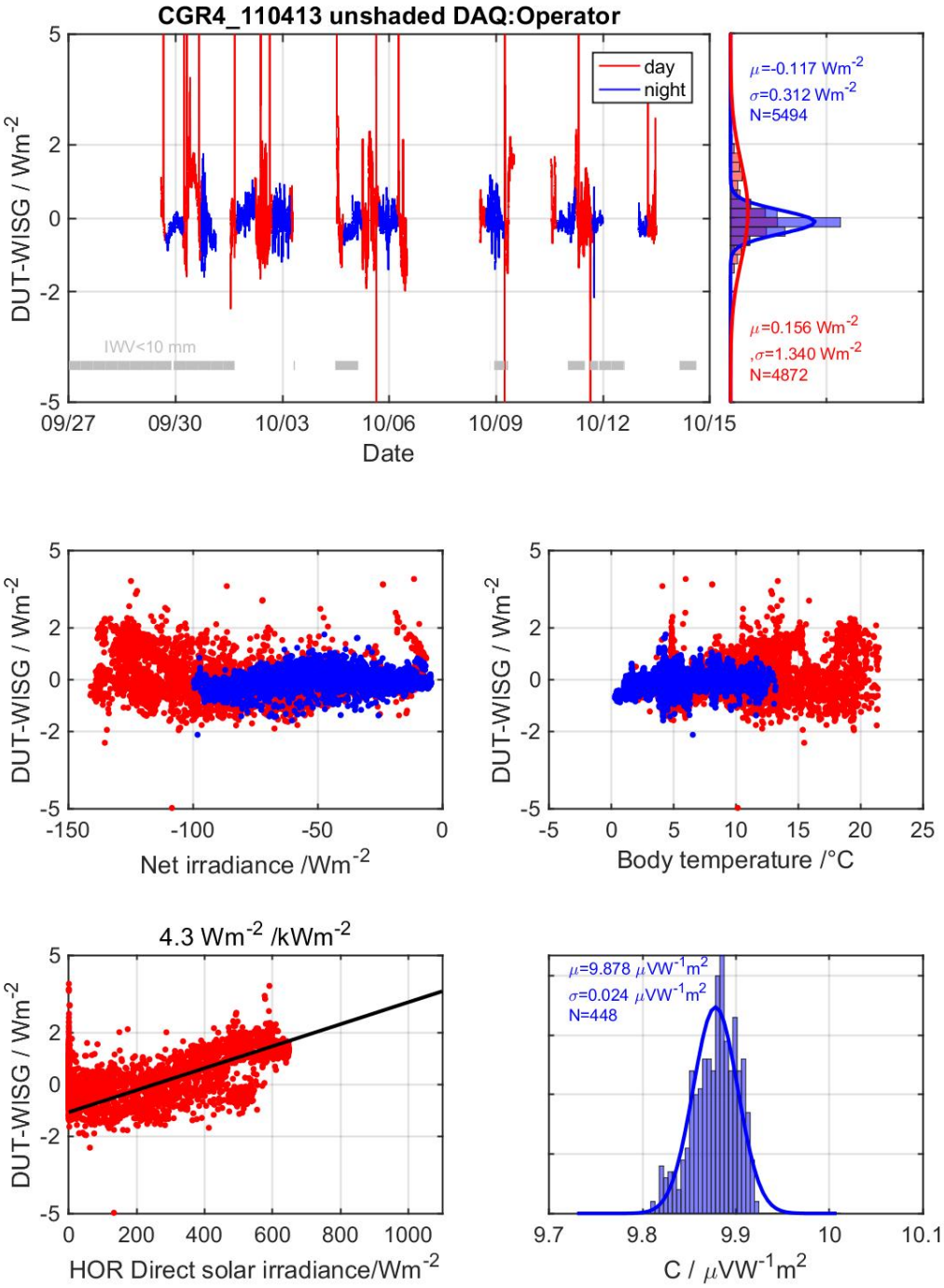
CGR4_110413 unshaded DAQ:Operator
DUT-WISG / Wm-2
day
night
IWV<10 mm
μ=-0.117 Wm-2
σ=0.312 Wm-2
N=5494
μ=0.156 Wm-2
,σ=1.340 Wm-2
N=4872
09/27
09/30
10/03
10/06
10/09
10/12
10/15
Date
Net irradiance /Wm-2
Body temperature /°C
4.3 Wm-2 /kWm-2
HOR Direct solar irradiance/Wm-2
μ=9.878 μVW-1m2
σ=0.024 μVW-1m2
N=448
C / μVW-1m2

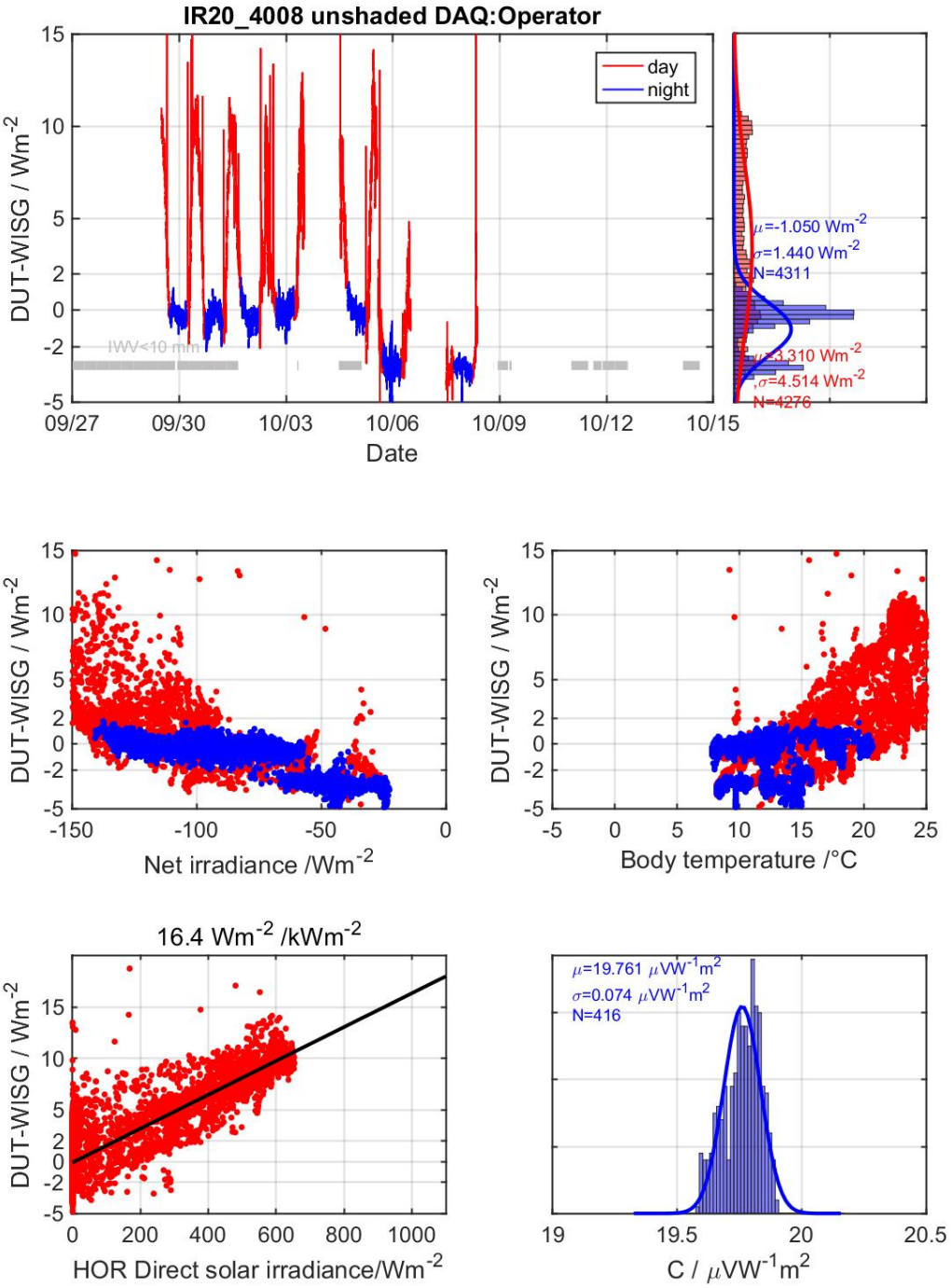
IR20_4008 unshaded DAQ:Operator
DUT-WISG / Wm-2
day
night
IWV<10 mm
μ=-1.050 Wm-2
σ=1.440 Wm-2
N=4311
μ=3.310 Wm-2
σ=4.514 Wm-2
N=4276
09/27
09/30
10/03
10/06
10/09
10/12
10/15
Date
Net irradiance /Wm-2
Body temperature /°C
16.4 Wm-2 /kWm-2
HOR Direct solar irradiance/Wm-2
μ=19.761 μVW-1m2
σ=0.074 μVW-1m2
N=416
C / μVW-1m2

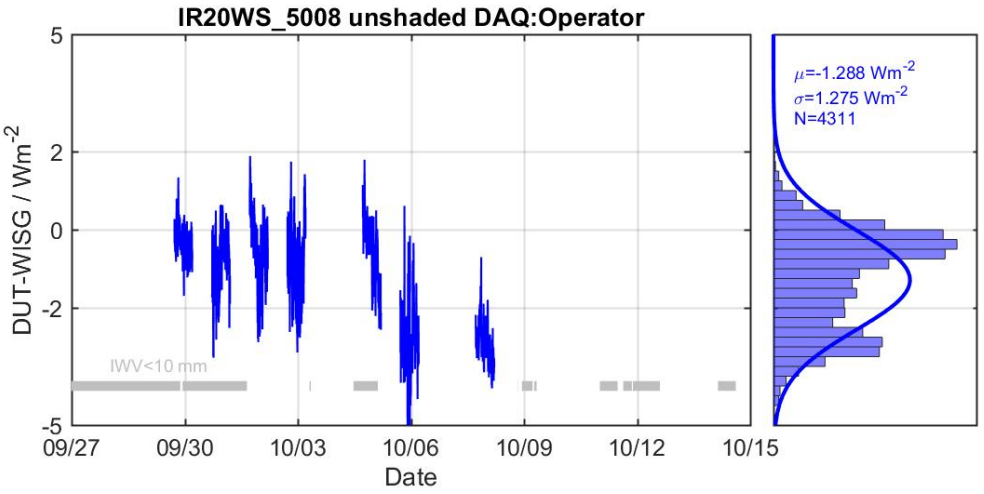
IR20WS_5008 unshaded DAQ:Operator
DUT-WISG / Wm-2
IWV<10 mm
09/27
09/30
10/03
10/06
10/09
10/12
10/15
Date
μ=-1.288 Wm-2
σ=1.275 Wm-2
N=4311

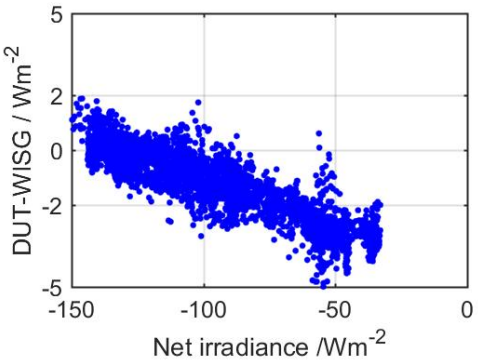
DUT-WISG / Wm-2
Net irradiance /Wm-2

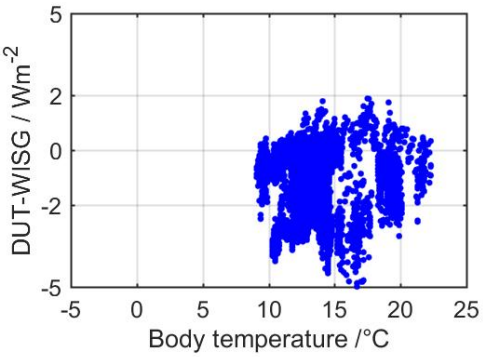
DUT-WISG / Wm-2
Body temperature /°C

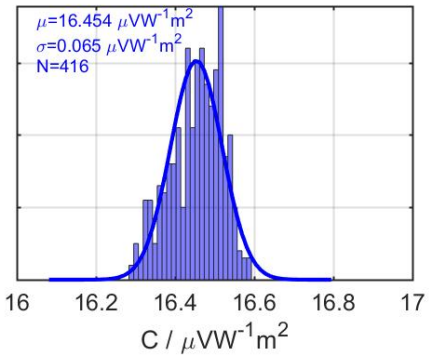
μ=16.454 μVW-1m2
σ=0.065 μVW-1m2
N=416
C / μVW-1m2

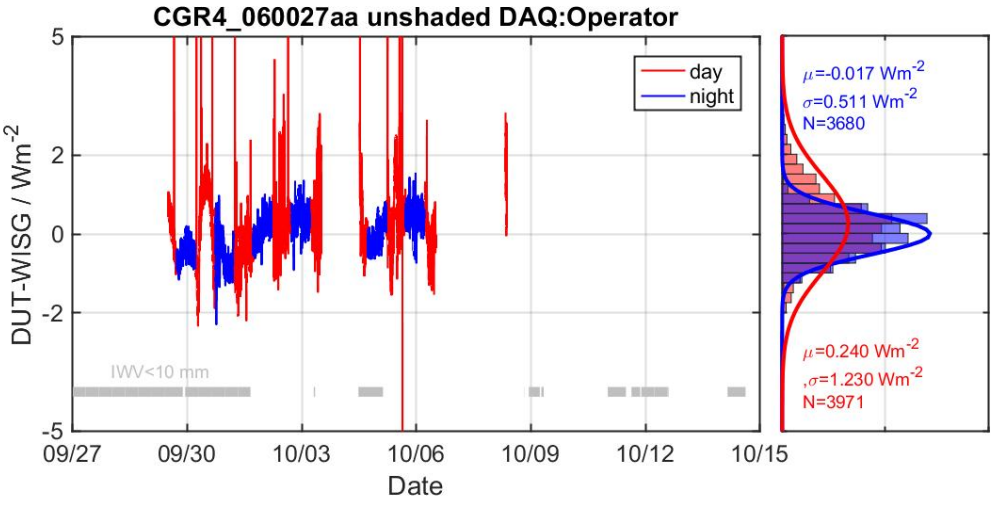
CGR4_060027aa unshaded DAQ:Operator
DUT-WISG / Wm-2
day
night
IWV<10 mm
μ=-0.017 Wm-2
σ=0.511 Wm-2
N=3680
μ=0.240 Wm-2
,σ=1.230 Wm-2
N=3971
09/27
09/30
10/03
10/06
10/09
10/12
10/15
Date

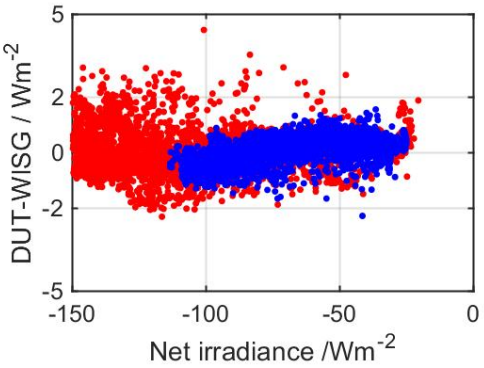
DUT-WISG / Wm-2
Net irradiance /Wm-2

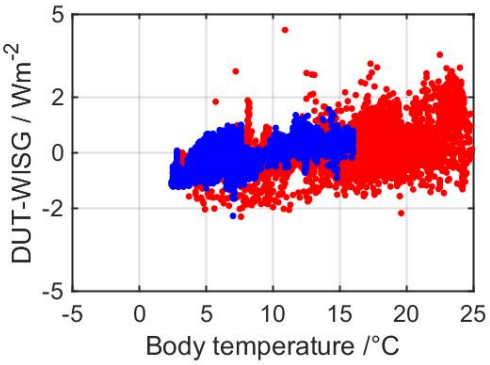
DUT-WISG / Wm-2
Body temperature /°C

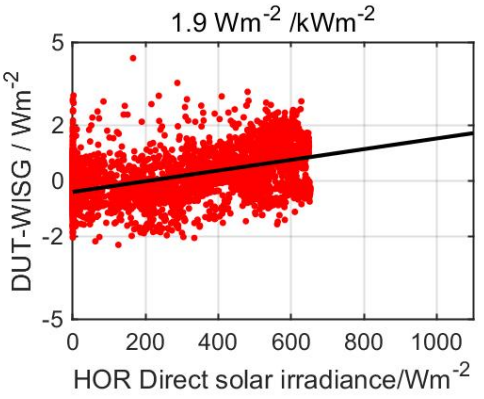
1.9 Wm-2 /kWm-2
DUT-WISG / Wm-2
HOR Direct solar irradiance/Wm-2

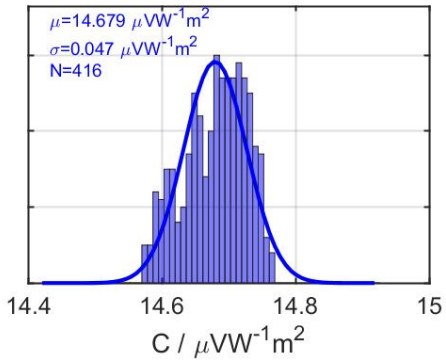
μ=14.679 μVW-1m2
σ=0.047 μVW-1m2
N=416
C / μVW-1m2

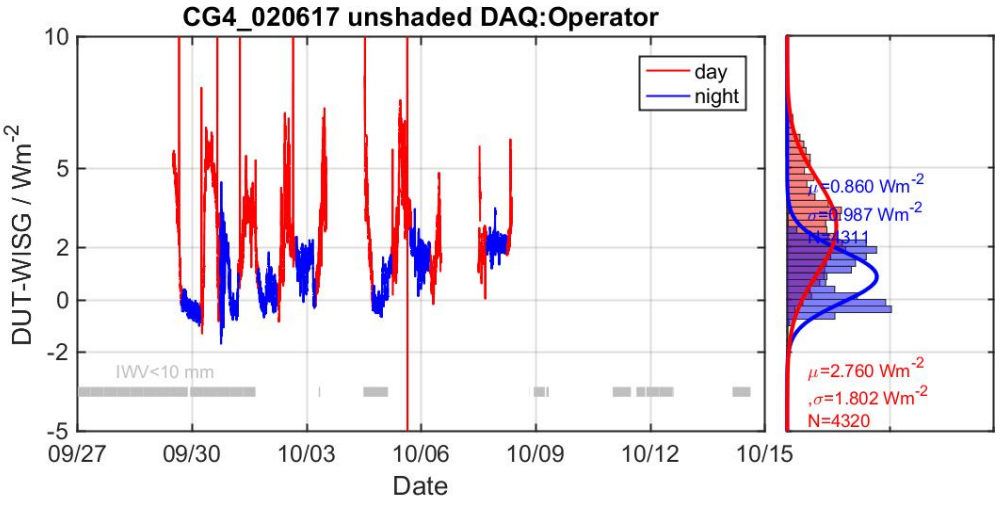
CG4_020617 unshaded DAQ:Operator
day
night
DUT-WISG / Wm-2
IWV<10 mm
09/27
09/30
10/03
10/06
10/09
10/12
10/15
Date
μ=0.860 Wm-2
σ=0.987 Wm-2
μ=2.760 Wm-2
σ=1.802 Wm-2
N=4320

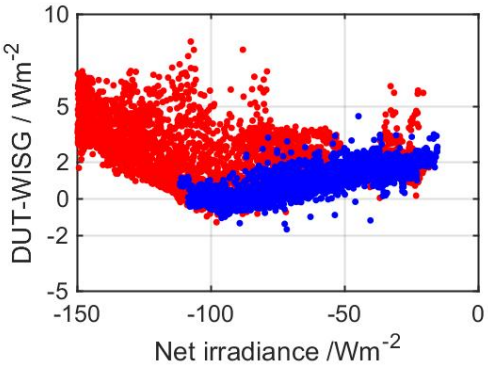
DUT-WISG / Wm-2
Net irradiance /Wm-2

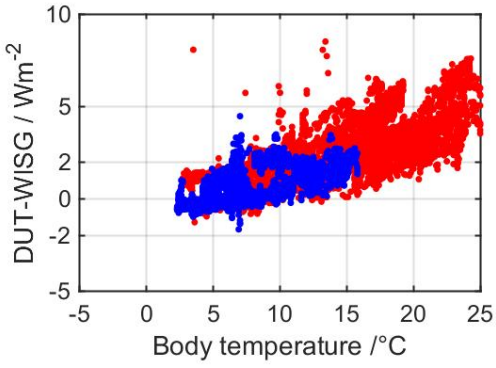
DUT-WISG / Wm-2
Body temperature /°C

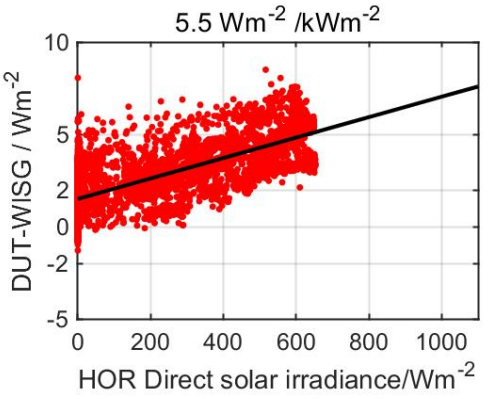
5.5 Wm-2 /kWm-2
DUT-WISG / Wm-2
HOR Direct solar irradiance/Wm-2

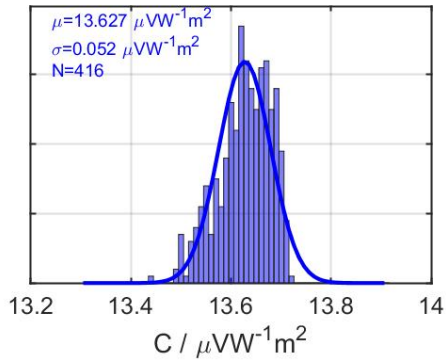
μ=13.627 μVW-1m2
σ=0.052 μVW-1m2
N=416
C / μVW-1m2

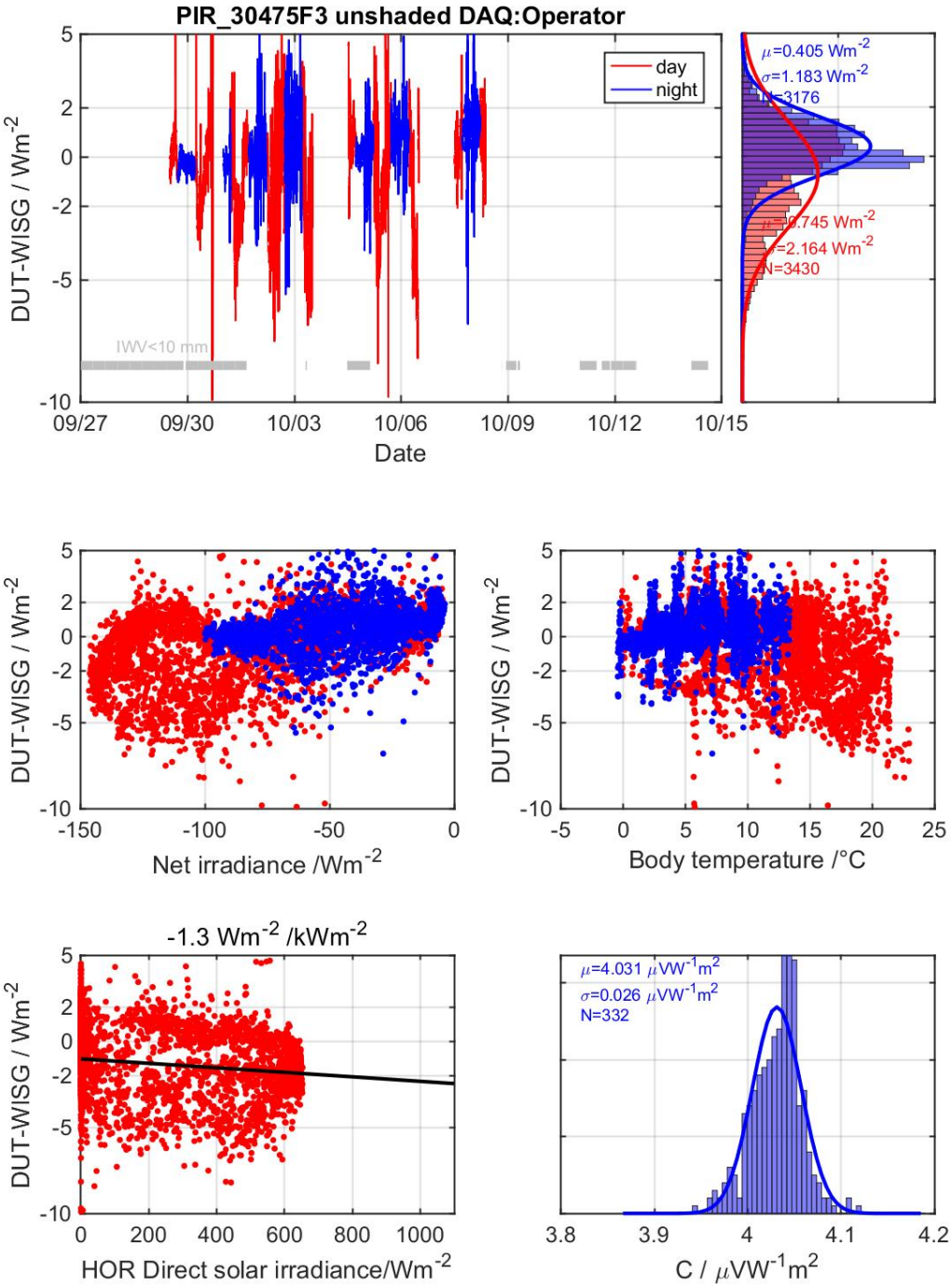
PIR_30475F3 unshaded DAQ:Operator
DUT-WISG / Wm-2
Date
day
night
IWV<10 mm
μ=0.405 Wm-2
σ=1.183 Wm-2
N=3176
μ=-0.745 Wm-2
σ=2.164 Wm-2
N=3430
Net irradiance /Wm-2
Body temperature /°C
-1.3 Wm-2 /kWm-2
HOR Direct solar irradiance/Wm-2
μ=4.031 μVW-1m2
σ=0.026 μVW-1m2
N=332
C / μVW-1m2

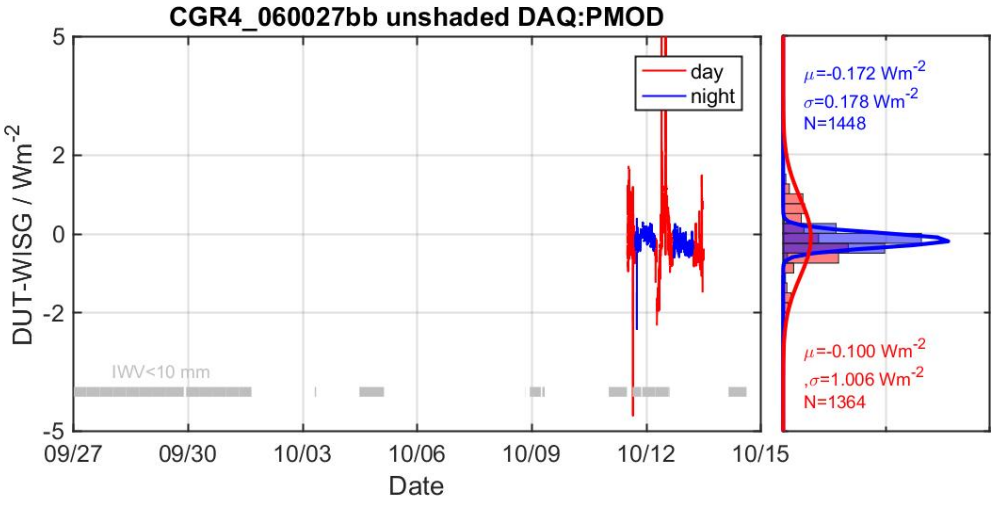
CGR4_060027bb unshaded DAQ:PMOD
day
night
μ=-0.172 Wm-2
σ=0.178 Wm-2
N=1448
μ=-0.100 Wm-2
,σ=1.006 Wm-2
N=1364
IWV<10 mm
DUT-WISG / Wm-2
Date
09/27
09/30
10/03
10/06
10/09
10/12
10/15

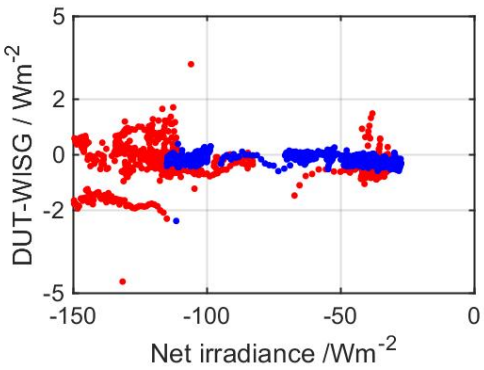
DUT-WISG / Wm-2
Net irradiance /Wm-2

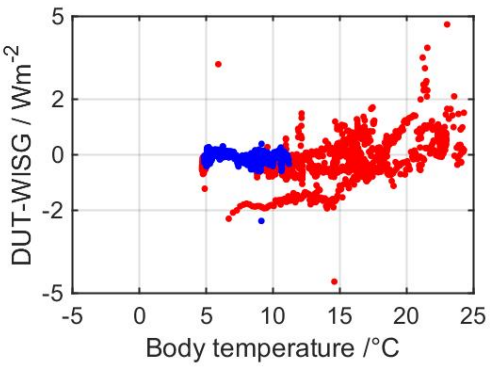
DUT-WISG / Wm-2
Body temperature /°C

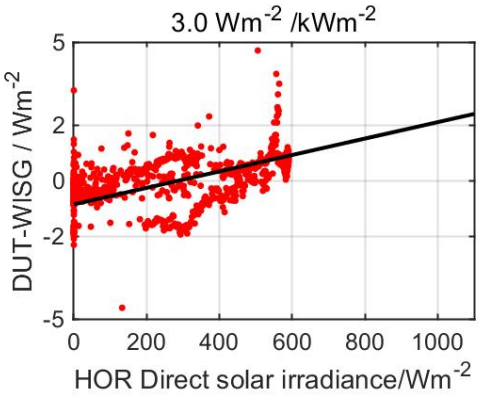
3.0 Wm-2 /kWm-2
DUT-WISG / Wm-2
HOR Direct solar irradiance/Wm-2

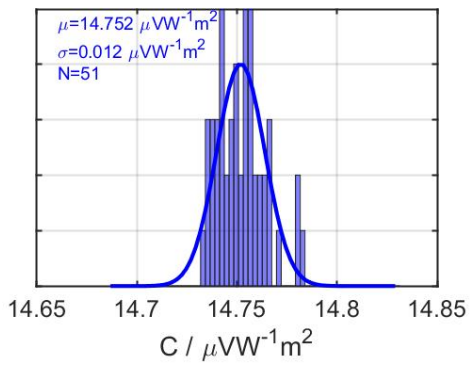
μ=14.752 μVW-1m2
σ=0.012 μVW-1m2
N=51
C / μVW-1m2

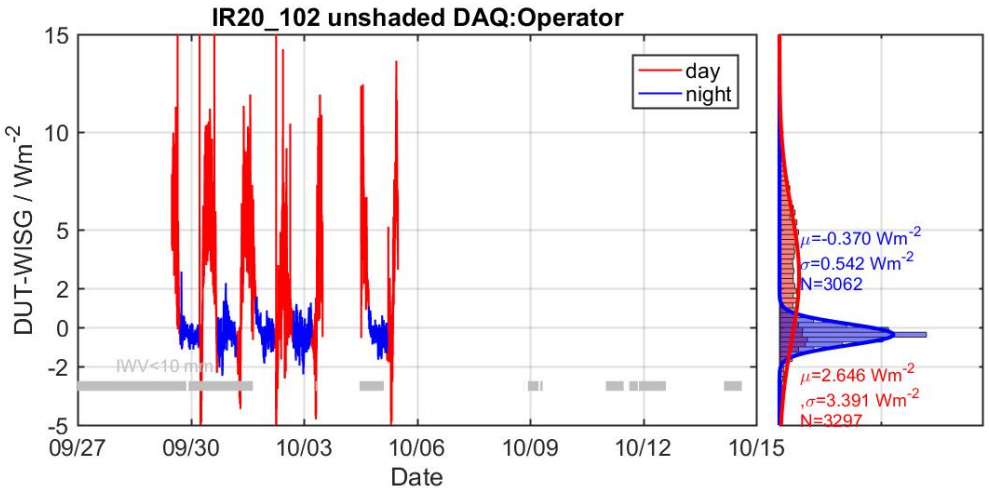
IR20_102 unshaded DAQ:Operator
day
night
DUT-WISG / Wm-2
IWV<10 mm
μ=-0.370 Wm-2
σ=0.542 Wm-2
N=3062
μ=2.646 Wm-2
,σ=3.391 Wm-2
N=3297
09/27
09/30
10/03
10/06
10/09
10/12
10/15
Date

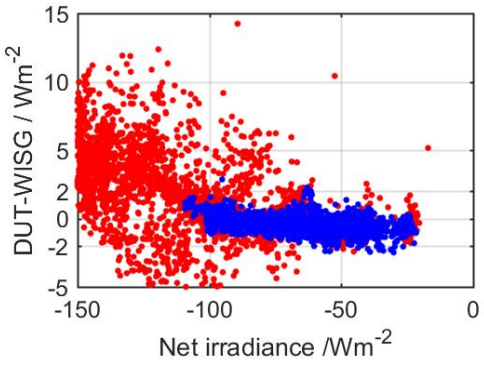
DUT-WISG / Wm-2
Net irradiance /Wm-2

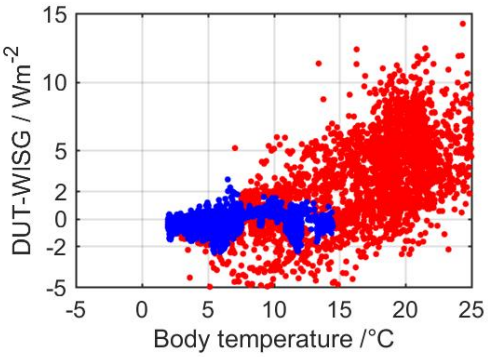
DUT-WISG / Wm-2
Body temperature /°C

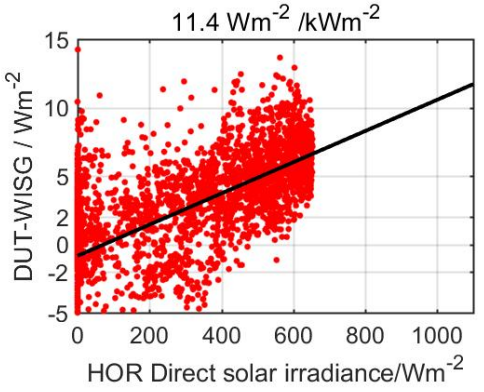
11.4 Wm-2 /kWm-2
DUT-WISG / Wm-2
HOR Direct solar irradiance/Wm-2

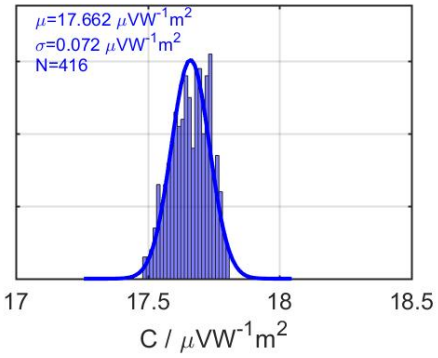
μ=17.662 μVW-1m2
σ=0.072 μVW-1m2
N=416
C / μVW-1m2

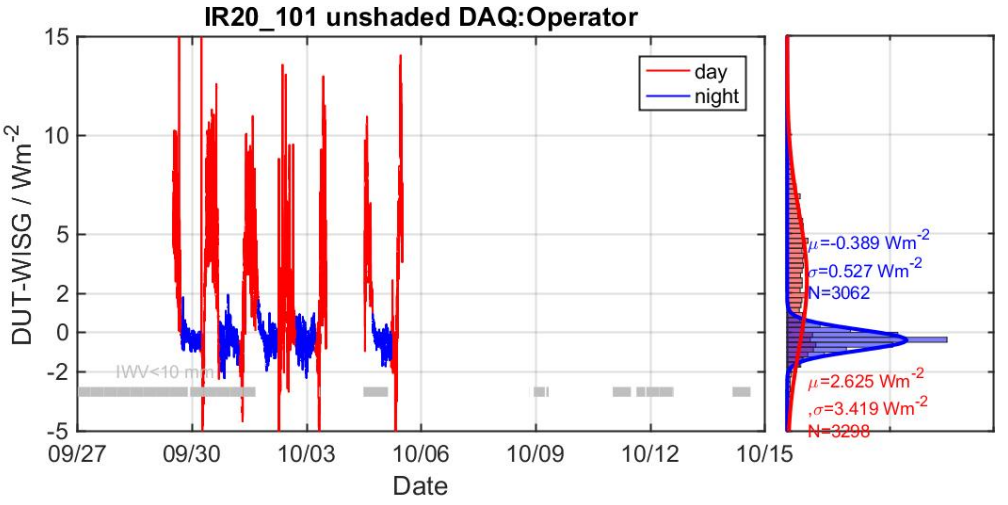
IR20_101 unshaded DAQ:Operator
DUT-WISG / Wm-2
Date
day
night
IWV<10 mm
μ=-0.389 Wm-2
σ=0.527 Wm-2
N=3062
μ=2.625 Wm-2
σ=3.419 Wm-2
N=3298

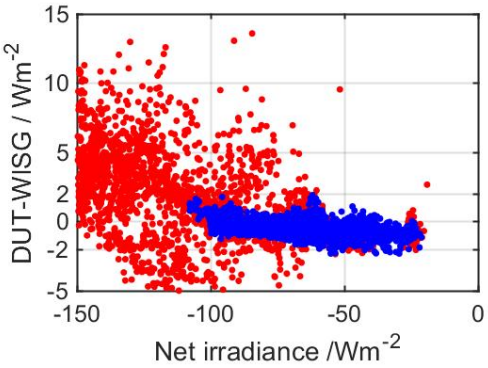
DUT-WISG / Wm-2
Net irradiance /Wm-2

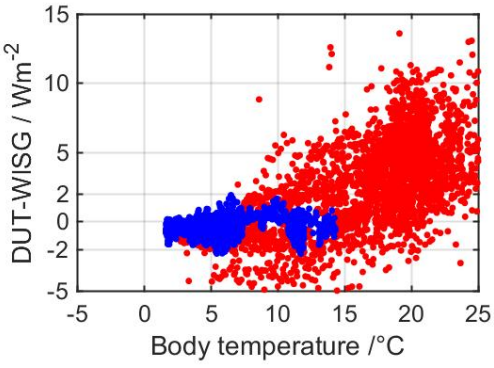
DUT-WISG / Wm-2
Body temperature /°C

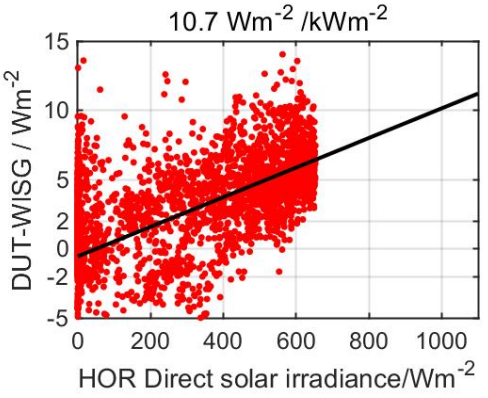
10.7 Wm-2 /kWm-2
DUT-WISG / Wm-2
HOR Direct solar irradiance/Wm-2

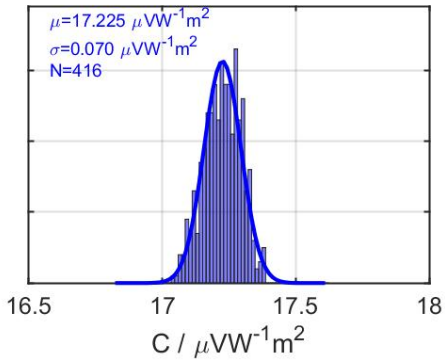
μ=17.225 μVW-1m2
σ=0.070 μVW-1m2
N=416
C / μVW-1m2

For more information, please contact:

World Meteorological Organization

7 bis, avenue de la Paix – P.O. Box 2300 – CH 1211 Geneva 2 – Switzerland

Communication and Public Affairs Office

Tel.: +41 (0) 22 730 83 14/15 – Fax: +41 (0) 22 730 81 71

E-mail: cpa@wmo.int

public.wmo.int